Science of the Total Environment 838 (2022) 156084

Contents lists available at ScienceDirect

Science of the Total Environment

journal homepage: www.elsevier.com/locate/scitotenv

Review

Emerging applications of high-precision Cu isotopic analysis by MC-ICP-MS

Kaj V. Sullivan [a,b,*], James A. Kidder [c], Tassiane P. Junqueira [a], Frank Vanhaecke [b], Matthew I. Leybourne [a,d]

[a] Department of Geological Sciences and Geological Engineering, Queens University, Kingston, ON, Canada
[b] Atomic & Mass Spectrometry – A&MS Research Unit, Department of Chemistry, Ghent University, Ghent, Belgium
[c] Geological Survey of Canada, Ottawa, Ontario, Canada
[d] Arthur B. McDonald Canadian Astroparticle Physics Research Institute, Department of Physics, Engineering Physics & Astronomy, Queen's University, Kingston, Ontario, Canada

HIGHLIGHTS

- Analytical protocols and methods for Cu isotopic analysis summarized
- Largest compilation of published δ^{65}Cu values for reference materials
- The Cu isotope ratio has potential as a vectoring tool for concealed ore deposits.
- Anthropogenic Cu tracing and biomonitoring possible with the Cu isotope ratio
- The Cu isotope ratio is a promising diagnostic and prognostic marker of disease.

GRAPHICAL ABSTRACT

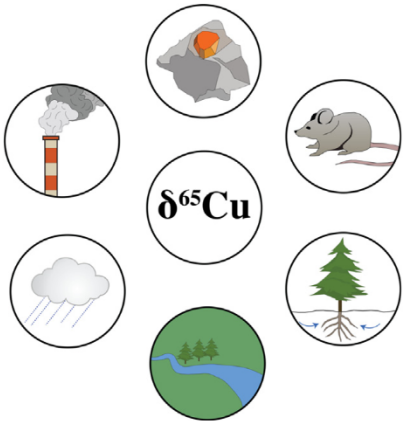

ARTICLE INFO

Editor: Mae Sexauer Gustin

Keywords:
Copper isotopes
δ^{65}Cu
MC-ICP-MS
Geochemistry
Mineral exploration
Isotope metallomics

ABSTRACT

As a component of many minerals and an essential trace element in most aerobic organisms, the transition metal element Cu is important for studying reduction-oxidation (redox) interactions and metal cycling in the total environment (lithosphere, atmosphere, biosphere, hydrosphere, and anthroposphere). The "fractionation" or relative partitioning of the naturally occurring "heavy" (^{65}Cu) and "light" (^{63}Cu) isotope between two coexisting phases in a system occurs according to bonding environment and/or as a result of a slight difference in the rate at which these isotopes take part in physical processes and chemical reactions (in absence of equilibrium). Due to this behaviour, Cu isotopic analysis can be used to study a range of geochemical and biological processes that cannot be elucidated with Cu concentrations alone. The shift between Cu^{+} and Cu^{2+} is accompanied by a large degree of Cu isotope fractionation, enabling the Cu isotope to be applied as a vector in mineral exploration, tracer of origin, transport, and fate of metal contaminants in the environment, biomonitor, and diagnostic/prognostic marker of disease, among other applications. In this contribution, we (1) discuss the analytical protocols that are currently available to perform Cu isotopic analysis, (2) provide a compilation of published δ^{65}Cu values for matrix reference materials, (3) review Cu isotope fractionation mechanisms, (4) highlight emerging applications of Cu isotopic analysis, and (5) discuss future research avenues.

* Corresponding author at: Ghent University, Department of Chemistry, Krijgslaan 281 – S12, B-9000 Ghent, Belgium.
E-mail address: kaj.sullivan@ugent.be (K.V. Sullivan).

http://dx.doi.org/10.1016/j.scitotenv.2022.156084
Received 21 March 2022; Received in revised form 16 May 2022; Accepted 16 May 2022
Available online 20 May 2022

Contents

1. Introduction . . . 2
2. Copper isotopic analysis . . . 3
   2.1. Instrumentation . . . 3
   2.2. Chromatographic Cu isolation . . . 4
   2.3. Correction for mass bias using sample-standard bracketing with internal normalization . . . 4
3. Quality assurance and quality control . . . 4
   3.1. Sources of metal contamination . . . 4
   3.2. Matrix reference materials. . . . 4
   3.3. Uncertainty estimation . . . 5
4. Copper isotope fractionation mechanisms . . . 5
   4.1. Mineral dissolution and precipitation . . . 5
   4.2. Adsorption . . . 7
   4.3. Biologically-mediated reactions . . . 8
5. Exploration geochemistry . . . 8
   5.1. Copper isotope ratio variations related to ore deposits. . . . 8
   5.2. Exploration hydrogeochemistry . . . 9
6. Tracing anthropogenic sources of Cu . . . 9
   6.1. Soils and surficial sediments . . . 9
   6.2. Vegetation . . . 10
   6.3. Aquatic settings . . . 10
   6.4. Cu stable isotopes as a biomonitoring tool . . . 11
7. Isotope metallomics . . . 11
   7.1. Breast cancer . . . 12
   7.2. Wilson's disease . . . 13
8. Conclusions . . . 13

Credit authorship contribution statement . . . 14
Acknowledgements . . . 14
Appendix A. Supplementary data . . . 14
References . . . 14

1. Introduction

The transition metal element Cu consists of two stable isotopes, ^{63}Cu and ^{65}Cu, and is an important element for studying reduction-oxidation (redox) interactions and metal cycling in the lithosphere, atmosphere, hydrosphere, biosphere, and anthroposphere (Fig. 1) (Moynier et al., 2017). Copper takes part in important redox reactions in the environment, shifting between Cu^{+} and Cu^{2+}, and as an essential trace element in most aerobic organisms, Cu is a useful tool for studying biological processes and metal dispersion in the environment (Kim et al., 2008; Uauy et al., 1998; Yruela, 2005).

The direction and intensity of changes in the abundance of Cu in a particular material or fluid cannot be quantitatively predicted (Télouk et al., 2015). However, this limitation can be overcome by the study of isotope fractionation between coexisting molecules, which can be quantitatively predicted by ab initio calculations (Fujii et al., 2013, 2014; Liu et al., 2021; Seo et al., 2007; Sherman, 2013; Sherman and Little, 2020; Tennant et al., 2017). The term "isotope fractionation" refers to the relative partitioning of the "heavy" (^{65}Cu) and "light" (^{63}Cu) isotope between two coexisting phases in a system. Because natural variations in the ratio (R), ^{65}Cu/^{63}Cu, are small, data are reported in δ^{65}Cu notation, which denotes the parts per thousand or "permille" (‰) change in the ^{65}Cu/^{63}Cu value of a sample relative to a Cu isotopic reference material used as a standard (Std; Eq. (1)).

$$\delta^{65}Cu_{Std} = \left(\frac{R^{65/63}_{Sample}}{R^{65/63}_{Std}} - 1\right) \cdot 1000 \quad (1)$$

Molecules containing the heavier isotope(s) of an element vibrate more slowly than the lighter forms, and because bond energy is inversely proportional to vibrational frequencies, heavy isotopes tend to preferentially occupy the lowermost energy levels (Albarède, 2015). In general, the strength of a particular bond is expected to be higher where the element is in a higher oxidation state (Cu^{2+}), where bond energy is split between fewer partners (lower coordination number), and when Cu is bound to more electronegative ligands (Albarède, 2015; Bigeleisen and Mayer, 1947).

Interest in high-precision Cu isotopic analysis has increased significantly over the last 20 years, translating into a large body of research spanning numerous fields (Bishop et al., 2012; Jaouen et al., 2013b; Mahan et al., 2020; Maréchal and Albarède, 2002; Maréchal et al., 1999; Moynier et al., 2017; Vanhaecke and Costas-Rodríguez, 2021; Wang et al., 2017, 2021; Wiederhold, 2015). Despite this, Cu has remained a relatively underused isotopic system in mineral exploration, environmental, and medical fields.

Recent research has demonstrated that the Cu isotope ratio can serve as a tracer of anthropogenic Cu contamination in surface and aquatic environments. Anthropogenic materials, such as cement, road dust, motor vehicle products, antifouling paint, Cu pesticides, flotation tailings, slag, urban aerosols, and particles originating from smelting and flue gas cleaning processes (Araújo et al., 2021b; Babcsányi et al., 2016; Blotevogel et al., 2018; Briant, 2014; Dong et al., 2017; El Azzi et al., 2013; Gelly et al., 2019; Gonzalez et al., 2016; Kříbek et al., 2018; Schleicher et al., 2020; Souto-Oliveira et al., 2018, 2019; Takano et al., 2020) are generally characterized by higher δ^{65}Cu values than those typical for geological materials (Araújo et al., 2019b; Liu et al., 2015; Savage et al., 2015; Wang et al., 2017).

Much opportunity also remains for the use of the Cu isotope ratio in groundwater as a mineral exploration vector. Recent research has shown relatively large surface and groundwater δ^{65}Cu dispersion haloes around mineral deposits that lack surface expression and cannot be revealed with Cu concentrations (Kidder et al., 2021, 2022; Mathur et al., 2013, 2014; Su et al., 2018). Much in the same way that the oxidative dissolution of Cu sulfide minerals can lead to Cu isotope fractionation in groundwater, the disruption of Cu homeostasis associated with many diseases (Brewer, 2003) can cause Cu isotope fractionation in blood compartments (Mahan et al., 2020; Vanhaecke and Costas-Rodríguez, 2021). In this newly-

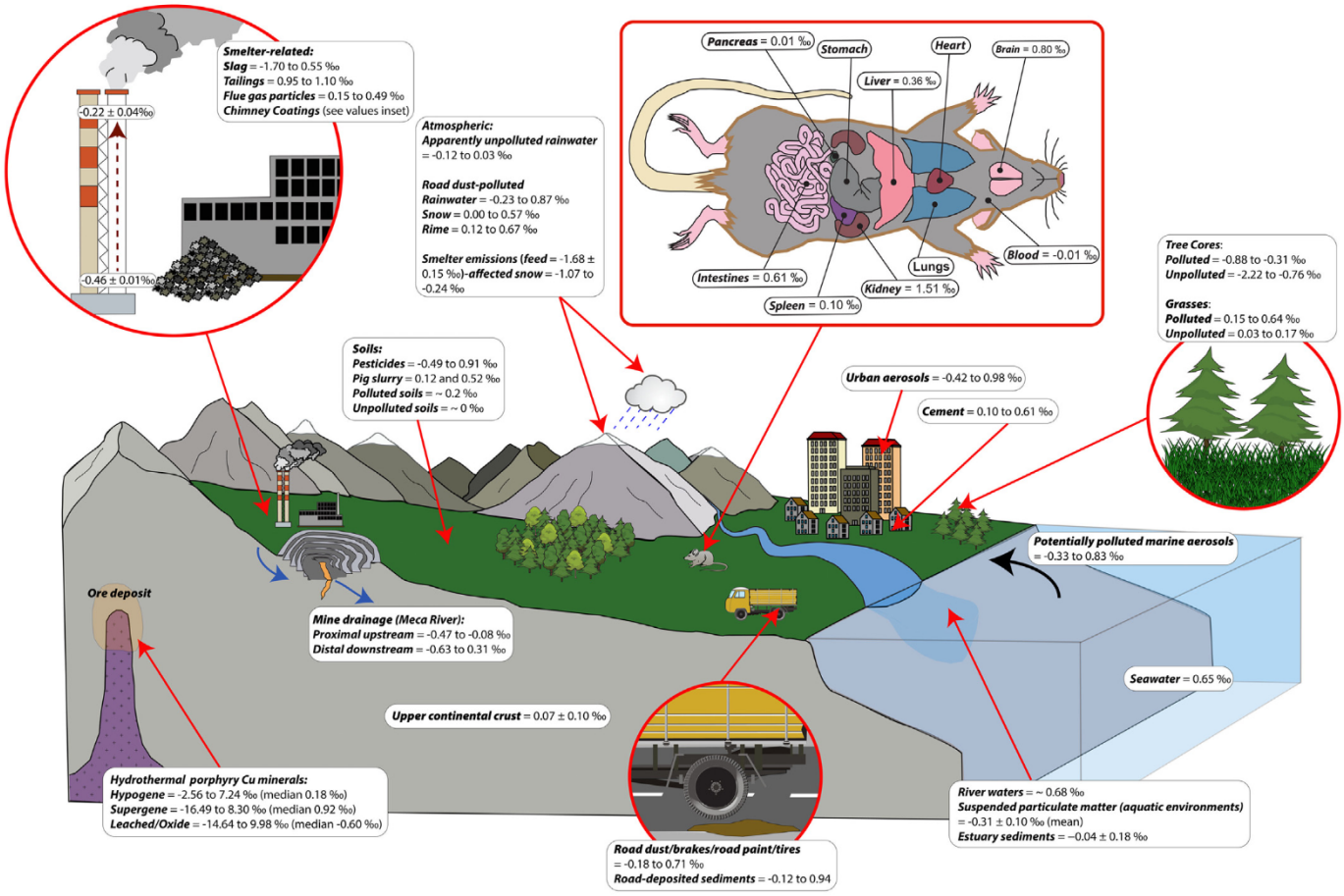

Fig. 1. Summary of the influence of natural and anthropogenic processes on the distribution of Cu stable isotopes in the environment. Data for/from: *smelter-related material* (Briant, 2014; Gelly et al., 2019; Křibek et al., 2018; Souto-Oliveira et al., 2018); *atmospheric samples* (Šillerová et al., 2017; Takano et al., 2014, 2021); *soils* (Babcsányi et al., 2016; Blotevogel et al., 2018; Chen et al., 2008; El Azzi et al., 2013; Fekiacova et al., 2015; Petit et al., 2013); *mouse* (Balter et al., 2013); *urban aerosols* (Schleicher et al., 2020); *cement* (Souto-Oliveira et al., 2018, 2019); *road-deposited sediments* (Jeong and Ra, 2021); *tree cores and grasses* (Křibek et al., 2018; Mihaljevič et al., 2018); *potentially polluted marine aerosols* (Takano et al., 2020); *seawater* (Little et al., 2018); *river waters* (Vance et al., 2008); *suspended particulate matter in aquatic environments* (Wang et al., 2017); *estuary sediments* (Araújo et al., 2019b); *upper continental crust* (Liu et al., 2015; Savage et al., 2015); *mine drainage* (Masbou et al., 2020); *hydrothermal porphyry Cu deposits* (Braxton and Mathur, 2011; Graham et al., 2004; Li et al., 2010; Mathur et al., 2009, 2010, 2012, 2013; Mirnejad et al., 2010; Palacios et al., 2011; Wu et al., 2017).

named field of research, isotope metallomics, stable metal isotope techniques are applied to biomedicine, and the Cu isotope ratio has already been identified as a marker of multiple cancers and other diseases (Mahan et al., 2020; Vanhaecke and Costas-Rodríguez, 2021).

In this contribution, we review recent advances in Cu isotopic analysis with regards to (1) chromatographic isolation of Cu – particularly for samples with ultra-trace Cu concentrations, (2) analytical methods for Cu isotope ratio determination, (3) matrix reference materials, (4) processes that fractionate Cu isotopes, (5) hydrogeochemical mineral exploration, (6) tracing anthropogenic sources of Cu, and (7) isotope metallomics.

2. Copper isotopic analysis

2.1. Instrumentation

Measurements of the Cu isotope ratio were first performed using thermal ionization mass spectrometry (TIMS) (Shields et al., 1965; Walker et al., 1958). The advent of multi-collector inductively coupled plasma mass spectrometry (MC-ICP-MS) has improved the ability to process larger numbers of samples, but the instrumentation suffers from larger potential mass bias (preferential transmission of higher mass isotopes to the detectors), which requires correction (Archer and Vance, 2004; Maréchal et al., 1999; Yang et al., 2018; Zhu et al., 2000).

An MC-ICP-MS unit consists of an ICP ion source, mass analyzer, and an array of detectors. Although a relatively simple system, there are multiple potential sources of inaccuracy, including contamination, a low signal-to-noise ratio, temporal isotope fractionation drift, and isotope fractionation/mass bias during measurement (Yang et al., 2018). The causes of isotope fractionation/mass bias (or instrumental mass discrimination) during measurement are not fully understood, but are thought to occur from the supersonic expansion of the extracted ion cloud once it has passed through the sampler cone orifice, and from space-charge effects in and behind the skimmer cone region, both of which favour the transmission of the heavier isotope into the mass spectrometer (Yang et al., 2018). Desolvating interface sample introduction systems coupled to MC-ICP-MS may be used to perform measurements in dry plasma mode at a low flow rate with much-improved signal sensitivity, but there have been reports of measurement inaccuracy associated with the use of certain systems (Supplementary Information).

There has been limited utilization of laser ablation (LA)-MC-ICP-MS to determine the Cu isotope ratio in low-Cu samples. Two exceptions to this demonstrated the determination of the Cu isotope ratio in samples with complex matrices: directly in dried urine spots, and in dried spots of the solution obtained from the pre-treatment of serum by digestion and subsequent chromatographic isolation of Cu (García-Poyo et al., 2021; Resano et al., 2013). Potential Cu isotopic reference materials for LA-MC-ICP-MS were characterized by Yang et al. (2021).

2.2. Chromatographic Cu isolation

High-precision measurement of the Cu isotope ratio requires isolation of the target element with high yield (minimize the effect of on-column isotope fractionation, Supplementary Information) and analyte purity due to the effect of concomitant species on the extent of mass bias and the potential occurrence of spectral overlap caused by polyatomic ions (Hou et al., 2016; Liu et al., 2014; Maréchal et al., 1999; Yang et al., 2018). Of particular importance is the elimination of Na and Ti, which are the primary matrix components that need to be removed completely as they can produce polyatomic ions that interfere with the monitoring of the signals of ^{63}Cu and ^{65}Cu, including $^{40}Ar^{23}Na^{+}$, $^{23}Na_2^{16}O^1H$, $^{23}Na_2^{18}O^1H^{+}$, $^{47}Ti^{16}O^{+}$, $^{46}Ti^{16}O^1H^{+}$, $^{49}Ti^{16}O^{+}$, and $^{48}Ti^{16}O^1H^{+}$ (Hou et al., 2016). Therefore, Ti and Na levels in the Cu isolate should be determined by (single-collector) ICP-MS to determine Ti/Cu and Na/Cu values and ensure they are below approximately 0.3 and 0.5, respectively (Hou et al., 2016; Liu et al., 2014). Even the presence of elements that do not cause prominent spectral interferences with the signals of ^{63}Cu and ^{65}Cu can affect the raw MC-ICP-MS Cu isotope ratio data. For example, the effect of Co on $\delta^{65}Cu$ is significant when the Co-to-Cu ratio reaches 1 (Hou et al., 2016). Copper isotopic analysis without prior purification is possible in samples with very simple matrix compositions or in media with high Cu concentrations, such as Cu sulfide, sulfate, and oxide minerals (Balliana et al., 2013; Larson et al., 2003; Mathur et al., 2005, 2009; Zhang et al., 2020; Zhu et al., 2000). Chromatographic isolation of Cu can also be avoided when bracketing standards of known Cu isotopic composition are perfectly matrix-matched with samples (Hou et al., 2016).

The most significant development in Cu chromatography (and which most methods are based upon) came from Maréchal et al. (1999), who used the AG® MP-1 resin and 7 M HCl with 0.001% H_2O_2 to achieve high-purity Cu elutions. Further adaptions were needed for isolating Cu from fresh waters and those with high-salinity matrices, such as seawater (Bermin et al., 2006; Wang et al., 2020a; Yang et al., 2020). These methods employed the use of Cu-specific resins, Bio-Rad Chelex 100 (Bermin et al., 2006; Vance et al., 2008) and Nobias-PA1 (Little et al., 2018; Takano et al., 2013, 2017, 2020, 2021; Yang et al., 2020), to preconcentrate Cu prior to the purification step. However, these two resins require the sample pH to be adjusted to within a narrow range in order to quantitatively retain Cu on the column. Wang et al. (2020a) used CU resin (Eichrom Technologies Inc.), which quantitatively retains Cu over a wide pH range (about pH 4 to 9) to purify Cu from seawater. Given that most seawater has a pH of ~8, pH adjustment is not necessary. Nitrilotriacetic acid resin (NTA Superflow®) has also been employed for the preconcentration stage, with a peristatic pump to speed up the purification process (Baconnais et al., 2019). Additional innovations to Cu chromatography are discussed in the Supplementary Information.

Perhaps the biggest barrier to mainstream application of the Cu isotope ratio is the time required for sample preparation (namely, the isolation of Cu), which can potentially be reduced through the simplification of the Cu purification process and automation. To that end, automated ion-exchange chromatography systems, such as the prepFast-MC (ESI) and the Chemcob II (Analab), were developed. There are multiple benefits to these systems for separating low amounts of Cu (~100 ng) from complicated matrices (e.g., human serum and brines), with the removal of human operators from the method and procedures taking place in an enclosed and HEPA-filtered environment reducing the risk of sample contamination during ion-exchange chromatography. Other improvements include the high reproducibility of flow rates, sample and reagent volumes, and wash times. Such automated methods have been successfully developed for Cu and several other isotope systems, including Sr, Nd, Pb, and Ca (Enge et al., 2016; Kidder et al., 2020; Meynadier et al., 2006; Retzmann et al., 2017; Romaniello et al., 2015; Schmitt et al., 2009).

2.3. Correction for mass bias using sample-standard bracketing with internal normalization

An external standard with known Cu isotopic composition measured in a sample-standard bracketing (SSB) approach is commonly used to correct not only for mass bias, but also for instrumental drift during measurement, as it is based on sequential measurements of standard-sample-standard. The SSB correction is performed by calculating $\delta^{65}Cu$ using the raw (uncorrected) isotope ratio of the sample solution, the mean raw (uncorrected) isotope ratio of the bracketing standard measured immediately before and after the sample in the measurement sequence (Eq. (1)), and the known isotope ratio of the standard. As the corrected isotope ratio can show dependence on concentration, it is necessary to match the Cu concentration in the sample and the bracketing standard to within 10% to ensure accurate isotope ratio measurements (Liu et al., 2014; Petit et al., 2008; Yang et al., 2018). By convention, $\delta^{65}Cu$ values are reported relative to National Institute of Standards and Technology (NIST) Standard Reference Material (SRM) 976, but other isotopic reference materials are available (Supplementary Information).

Temporal, and to some extent, matrix-induced drifts in instrumental isotope fractionation are unable to be fully corrected for using an external correction in an SSB approach, but this can be overcome with the use of another element as an internal standard (Yang et al., 2018). A combination of external correction and internal normalization (C-SSBIN) mass bias correction using Ga as an internal standard is the preferred method to correct for instrumental mass bias for Cu, as it corrects for temporal drifts and provides a better measurement uncertainty than SSB alone (Hou et al., 2016; Yang et al., 2018). Other calibrants, such as Zn (Maréchal et al., 1999) or Ni (Ehrlich et al., 2004), can be used, but Ga isotopes have no isobaric interferents and less polyatomic interferents (Hou et al., 2016). Gallium is also less abundant than Zn and Ni in the Earth's crust and therefore has fewer sources of contamination. As with the analyte, Cu, Ga concentrations in the sample and the bracketing standard must also be matched to within 10% to minimize the effect of concentration dependence on corrected isotope ratios (Liu et al., 2014; Yang et al., 2018). Significant instrumental drift effects during Cu isotopic analysis by LA-MC-ICP-MS cannot be corrected with SSB alone (Yang et al., 2021). The C-SSBIN mass bias correction method can also be employed during LA-MC-ICP-MS by admixing a "semi-dry" aerosol of Zn, generated by an Aridus II™ desolvating nebulization system (CETAC, Omaha, United States) to the ablation aerosol (Yang et al., 2021). The calculation of the mass bias-corrected sample $^{65}Cu/^{63}Cu$ value is described in Sullivan et al. (2020a). The value obtained for the internal standard isotope ratio may be biased due to the limitations of the isotope fractionation correction model (e.g., $f_{Cu} = f_{Ga}$), but this is largely negated in the second step of the calibration from Ga → Cu (Yang et al., 2018). The relationship between the mass bias correction factors, f_{Cu} and f_{Ga}, is taken into account in the correction model of Baxter et al. (2006).

3. Quality assurance and quality control

3.1. Sources of metal contamination

Laboratory materials, such as gloves and bottles, have been investigated as a source of Cu contamination (Duangthong et al., 2017; Friel et al., 1996; Gasparon, 1998), but significant metal contamination can also occur during sample collection. For example, blood collection tubes (BCTs) for separating serum/plasma from whole blood typically contain additives, such as citrate, silica gel, Na heparin, or dipotassium ethylenediaminetetraacetic acid (K_2EDTA), and are not prepared with the aim of trace element or isotopic analysis. However, BCTs specifically prepared for trace element analysis are commercially available. The potential problem lies in the fact that biobanks are valuable sources of blood samples for research, but samples are often derived from studies with different objectives that did not take into consideration potential trace metal contamination. An investigation of trace metal contamination present in different BCTs would provide valuable information on which tubes are suitable to study which elements.

3.2. Matrix reference materials

The ideal matrix reference material is characterized by a similar mineralogy, organic matter content, and abundances of major, minor, and trace elements to those found in the sample material to be analyzed. In some

cases, isotopic studies put pure, single-element standards alongside samples though separation methods, but this is inadequate to fully validate $\delta^{65}Cu$ measurements in samples as it only serves as a monitor of Cu yield from ion-exchange resins and contamination (Mathur et al., 2013). The processing of well-characterized, suitably matrix-matched RMs alongside real samples prior to isotopic analysis ensures that acid digestion and column chromatography procedures are adequate for the material type being investigated and flags occurring problems.

Despite the tracing of natural and anthropogenic Cu sources in soil being the subject of numerous studies (discussed later), well-characterized soil reference materials are noticeably lacking, and basalt reference materials have typically been used instead (Kříbek et al., 2018; Mihaljevič et al., 2018, 2019). However, this is inadequate due to the comparatively lower Cu concentrations and high organic content of soils which complicates their digestion and Cu purification. There is also a paucity of Cu isotope ratio data available for aqueous reference materials, and this must be improved for the full potential of hydrogeochemical applications of Cu isotopic analysis to be unlocked. The catalog of biological reference materials characterized for $\delta^{65}Cu$ is improving, with several recent articles focusing on their measurement (Jeong et al., 2021; Sauzéat et al., 2021; Sullivan et al., 2020a). The Sauzéat et al. (2021) interlaboratory comparison was an important step for the isotope metallomics community and increased the number of biological reference materials characterized for $\delta^{65}Cu$. The success of this interlaboratory comparison should inspire further comparisons, which will be helpful for those studying the isotopic fractionation of Cu (and other elements) in different settings.

To the best of our knowledge, we have prepared the largest compilation of published $\delta^{65}Cu$ values for matrix reference materials (Supplementary Information, Table S1). The unweighted mean value of the means from each cited article is provided as the best estimate of $\delta^{65}Cu$ for each of the 28 (15 geological, 9 biological, and 4 aqueous) reference materials (Table 1). These reference materials also cover much of the variability of $\delta^{65}Cu$ in "natural" Earth surface materials, ranging from −0.25‰ (BCR-414, plankton) to 0.67‰ (SRM 1573a, tomato leaves) (Fig. 2). We do not provide an exhaustive list of reference materials characterized for $\delta^{65}Cu$, but instead focus on materials that have been analyzed by multiple laboratories over many years. We also provide data for reference materials with matrix types that are seeing increased attention in literature (soil, biological, and aqueous) but require further analyses.

Table 1
The $\delta^{65}Cu_{SRM\ 976}$ values of matrix reference materials covering a wide range of matrices. Full data provided in Supplementary Information, Table S1. 2SE = standard error of reported means multiplied by two. Typical 2s (standard deviation multiplied by two) precision of 0.05‰ reported by laboratories for $\delta^{65}Cu$ measurements. * 2s of measurements provided due to values only being available from a single study.

Reference material	Type	Studies (*n*)	Recommended $\delta^{65}Cu_{SRM\ 976}$ (‰)
BCR-1/2	Columbia River basalt	26	0.19 ± 0.02 2SE
BHVO-2	Hawaiian basalt	21	0.10 ± 0.02 2SE
BIR-1/1a	Icelandic basalt	16	0.02 ± 0.02 2SE
AGV-1/2	Guano Valley andesite	12	0.06 ± 0.03 2SE
GSP-2	Granodiorite	8	0.29 ± 0.02 2SE
Nod-P-1	Mn nodule	8	0.37 ± 0.07 2SE
Seronorm™ Trace Elements Serum L-1	Human serum	7	−0.20 ± 0.05 2SE
MESS-3/4	Marine sediment	5	0.01 ± 0.12 2SE
PACS-2/3	Marine sediment	5	0.03 ± 0.08 2SE
DORM-4	Fish protein	5	0.53 ± 0.08 2SE
TORT-2/3	Lobster hepatopancreas	4	0.39 ± 0.09 2SE
W-2a	Diabase	4	0.09 ± 0.04 2SE
BCR-414	Plankton	3	−0.25 ± 0.06 2SE
SLRS-5	St Lawrence river water	3	0.38 ± 0.12 2SE
SRM 1566b	Oyster tissue	3	0.26 ± 0.04 2SE
SGR-1/1b	Green River shale	2	0.33 ± 0.08 2SE
ERM-CC141	Loam soil	2	0.51 ± 0.45 2SE
DOLT-4/5	Dogfish liver	2	−0.11 ± 0.17 2SE
ERM-CE278	Mussel tissue	2	0.22 ± 0.11 2SE
SRM 2976	Mussel tissue	2	0.20 ± 0.11 2SE
CASS-5	Near-shore seawater	2	0.46 ± 0.01 2SE
NASS-6	Seawater	2	0.42 ± 0.04 2SE
SRM 1573a	Tomato leaves	2	0.67 ± 0.07 2SE
GBW07443 (GSF-3)	Paddy soil	1	−0.04 ± 0.04 2s
GBW07425 (GSS-11)	Liaohe Plain soil	1	−0.07 ± 0.05 2s
GBW07427 (GSS-13)	North China Plain soil	1	−0.06 ± 0.04 2s
GBW07389 (GSS-33)	Floodplain sediments	1	−0.02 ± 0.06 2s
Trace Metals 1	Seawater	1	−0.21 ± 0.08 2s

3.3. Uncertainty estimation

Until recently, the precision of a sample measurement has commonly been reported as two standard deviations of repeated observations (from either the bracketing standard or a sample solution). However, the calculation of the combined uncertainty accompanying a determined $\delta^{65}Cu$ value accounts for the uncertainties of both the sample and bracketing standard isotope ratios and is quickly becoming the norm. The combined uncertainty associated with $\delta^{65}Cu$ measurements should be estimated in accordance with JCGM 2008 "Guide to the Expression of Uncertainty in Measurement", using the law of propagation of uncertainty. A full demonstration of the calculation of the combined uncertainty of $\delta^{65}Cu$ is provided by Sullivan et al. (2020a). Sullivan et al. (2020a) and Sauzéat et al. (2021) achieved comparable mean expanded uncertainties of ±0.07‰ and ±0.05‰ (U, k = 2), respectively, for measurements performed on a range of geological and biological reference materials.

4. Copper isotope fractionation mechanisms

A number of Cu isotope fractionation mechanisms play a role in the distribution of the Cu isotopes in the natural Earth surface environment, including reduction-oxidation reactions, adsorption onto mineral surfaces and organic complexation, and biologically-mediated reactions. Moynier et al. (2017) provided a comprehensive review of Cu stable isotope fractionation mechanisms, which include equilibrium (isotope fractionation between substances in chemical equilibrium) and kinetic (isotope fractionation from incomplete or unidirectional processes, e.g., microbial uptake) isotope effects; these mechanisms and recent advances in our understanding of them will be discussed insofar as they are relevant to the scope of this review. Figs. 3 and 4 provide a summary of the preference of each of these mechanisms for ^{63}Cu or ^{65}Cu and visualize how these preferences manifest themselves in the environment.

4.1. Mineral dissolution and precipitation

The largest variations in the Cu isotope ratio typically occur during phase changes associated with mineral dissolution and precipitation (Moynier et al., 2017). These are facilitated by redox reactions, with Cu shifting between the Cu^+ and Cu^{2+} oxidation states, providing potential as a tracer of sources and processes (Moynier et al., 2017). The oxidation of Cu sulfide minerals (chalcopyrite, bornite, and covellite) through interaction with natural waters produces large degrees of Cu isotope fractionation (up to 3.5‰), with the heavier isotope, ^{65}Cu, concentrated in the aqueous Cu^{2+} state (Asael et al., 2007; Fernandez and Borrok, 2009; Haest et al., 2009; Kimball et al., 2009; Mathur et al., 2005). In the dissolved phase of natural waters, the dominant form of Cu^{2+} binding is in strong, organic inner sphere complexes that are enriched in ^{65}Cu (Moynier et al., 2017).

A large degree of Cu isotope fractionation accompanies the reduction of Cu^{2+} to Cu^+ (Ehrlich et al., 2004; Qi et al., 2019). For example, a fractionation factor of 3.06 ± 0.14‰ ($\Delta^{65}Cu_{Cu(II)aq\ -\ CuS} = \delta^{65}Cu_{Cu(II)aq} -$

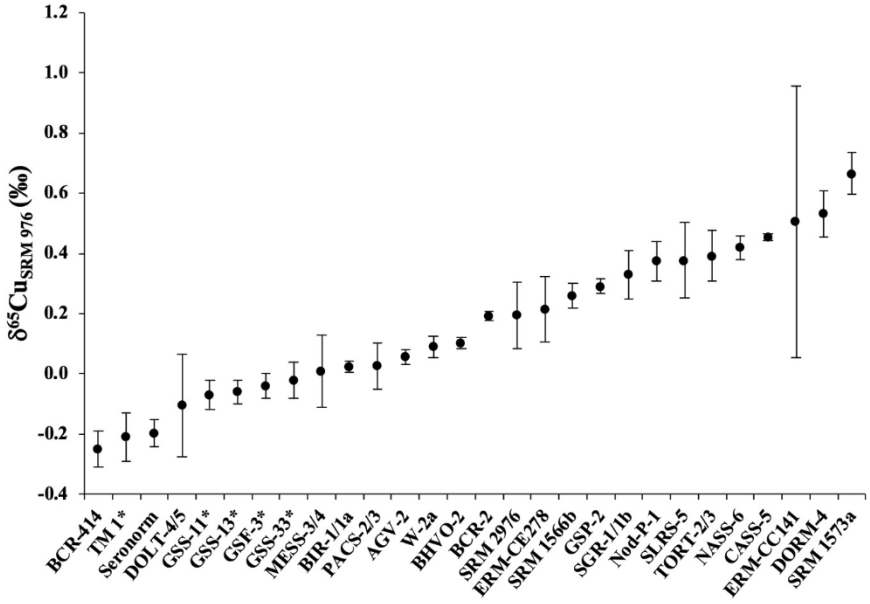

Fig. 2. Visualization of reference material $\delta^{65}Cu_{SRM\ 976}$ values (bars represent standard error of reported means multiplied by two (2SE) of $\delta^{65}Cu$ values from each study). * 2s of measurements provided due to values only being available from a single study.

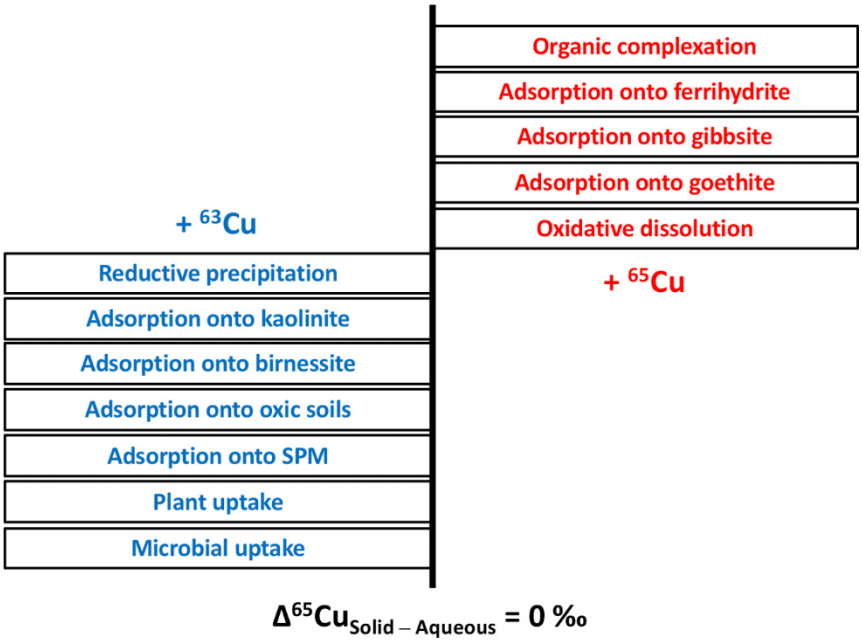

Fig. 3. Summary of the ^{65}Cu isotope enrichment/depletion patterns resulting from different Cu isotope fractionation mechanisms. Data for/from: *organic complexation* (Bigalke et al., 2010c; Ryan et al., 2014); *adsorption onto ferrihydrite* (Balistrieri et al., 2008); *adsorption onto gibbsite* (Pokrovsky et al., 2008); *adsorption onto goethite* (Pokrovsky et al., 2008); *oxidative dissolution* (Asael et al., 2007; Fernandez and Borrok, 2009; Haest et al., 2009; Kimball et al., 2009; Mathur et al., 2005); *reductive precipitation* (Ehrlich et al., 2004; Pękala et al., 2011; Qi et al., 2019); *adsorption onto kaolinite* (Li et al., 2015); *adsorption onto birnessite* (Ijichi et al., 2018; Little et al., 2014b; Sherman and Little, 2020); *adsorption onto oxic soils* (Vance et al., 2016); *adsorption onto suspended particulate matter (SPM)* (Vance et al., 2008; Wang et al., 2017); *plant uptake* (Blotevogel et al., 2019, 2022; Jouvin et al., 2012; Li et al., 2016, 2020; Navarrete et al., 2011b; Ryan et al., 2013; Weinstein et al., 2011; Wiggenhauser et al., 2022; Zheng et al., 2005; Zhu et al., 2010); *microbial uptake* (Mathur et al., 2005; Navarrete et al., 2011a; Pokrovsky et al., 2008; Zhu et al., 2002). Adapted after Komárek et al. (2021) and Moynier et al. (2017).

$\delta^{65}Cu_{CuS}$) is reported for the precipitation of covellite ($Cu^{+}S$) from the reduction of aqueous Cu^{2+} during laboratory experiments (Ehrlich et al., 2004). However, under special conditions, results can be yielded that contradict this. For instance, during the initial stage of supergene alteration in the Spence Cu-Mo porphyry system (Chile), the oxidation and leaching of hypogene Cu sulfides by infiltrating meteoric water in a semi-arid climate lead to the precipitation of secondary chalcocite at the redox front with $\delta^{65}Cu$ values ranging from 3.91 to 3.95‰, which represents fractionation of ~3.6‰ from the hypogene sulfides (Palacios et al., 2011).

The effects of temperature on the degree of Cu isotope fractionation in reduction reactions have also been the subject of investigation. Qi et al. (2019) reported a $\Delta^{65}Cu_{Cu(0)-Cu(II)}$ of −2.66‰ at 35 °C and −1.93‰ at 80 °C, suggesting an inverse dependence of isotope fractionation on temperature, but at 5 °C, mass transport (diffusion) appears to dominate over

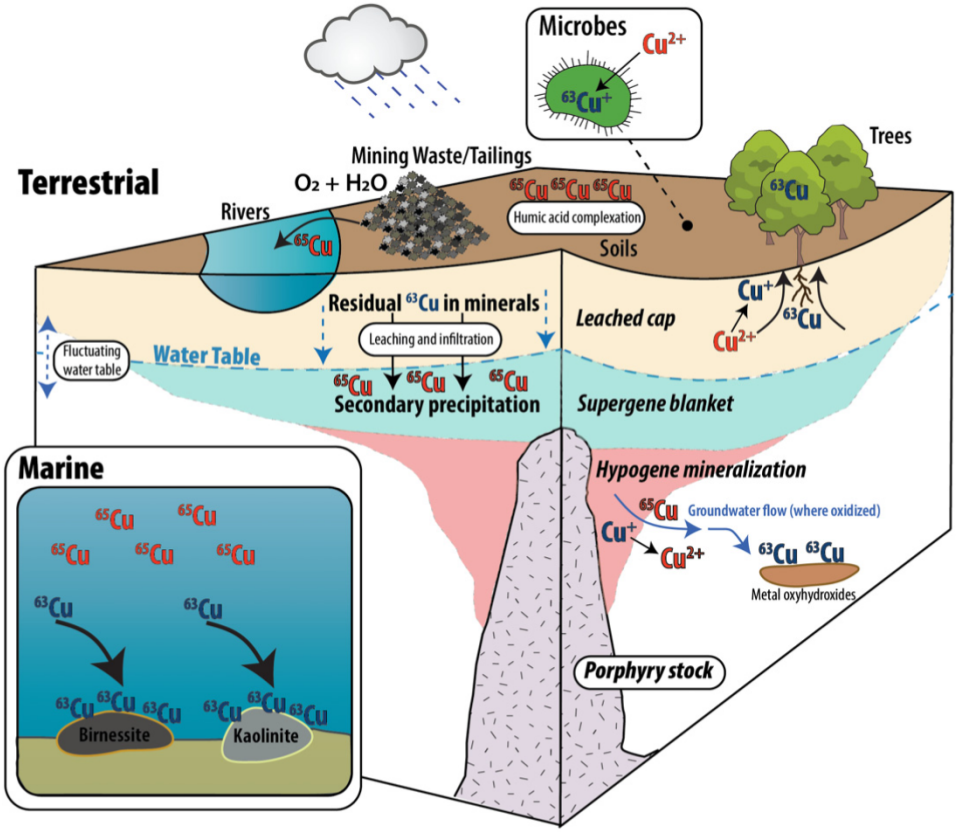

Fig. 4. Visualization of the ^{65}Cu isotope enrichment/depletion patterns resulting from different Cu isotope fractionation mechanisms in the environment. Data for/from: *organic acid complexation* (Bigalke et al., 2010c; Ryan et al., 2014); *adsorption onto ferrihydrite* (Balistrieri et al., 2008); *adsorption onto gibbsite* (Pokrovsky et al., 2008); *adsorption onto goethite* (Pokrovsky et al., 2008); *oxidative dissolution* (Asael et al., 2007; Fernandez and Borrok, 2009; Haest et al., 2009; Kimball et al., 2009; Mathur et al., 2005); *adsorption onto kaolinite* (Li et al., 2015); *adsorption onto birnessite* (Ijichi et al., 2018; Little et al., 2014b; Sherman and Little, 2020); *plant uptake* (Blotevogel et al., 2019, 2022; Jouvin et al., 2012; Li et al., 2016, 2020; Navarrete et al., 2011b; Ryan et al., 2013; Weinstein et al., 2011; Wiggenhauser et al., 2022; Zheng et al., 2005; Zhu et al., 2010); *microbial uptake* (Mathur et al., 2005; Navarrete et al., 2011a; Pokrovsky et al., 2008; Zhu et al., 2002).

reaction kinetics, which results in a smaller degree of fractionation (−1.21‰). Pękala et al. (2011) reported $\Delta^{65}Cu_{Solution\ -\ Mineral}$ values ranging from 1.97 to 3.23‰ (average of 2.64‰) for the reaction of aqueous Cu^{2+} with Fe^{2+} sulfide minerals (pyrrhotite and pyrite), and concluded that significant fractionation is possible at moderate temperatures of 150 to 200 °C.

4.2. Adsorption

Trends for Cu isotope fractionation during adsorption are more nuanced. At pH 4 to 6, ^{65}Cu is preferentially adsorbed onto the metal oxyhydroxide minerals, gibbsite and goethite (Pokrovsky et al., 2008). Similarly, ^{65}Cu is also preferentially adsorbed onto the surface of amorphous Fe^{3+} oxyhydroxide phases (Balistrieri et al., 2008). This preference of ^{65}Cu during adsorption onto metal oxyhydroxide minerals is most likely the result of a change in bond length and coordination from six-fold coordination in solution to four-fold coordination when adsorbed (Pokrovsky et al., 2008).

Conversely, the light isotope, ^{63}Cu, is preferentially adsorbed onto the surface of kaolinite (important Cu sink that is the second most abundant clay mineral in marine sediments), the Mn oxide mineral birnessite (primary mineral phase adsorbing divalent trace metals in ocean Fe-Mn crusts), suspended particulate matter (SPM), and oxic soil (Ijichi et al., 2018; Li et al., 2015; Little et al., 2014b; Sherman and Little, 2020; Takano et al., 2021; Vance et al., 2008, 2016). The mechanism behind the preferential adsorption of ^{63}Cu onto SPM and oxic soils remains unclear, but was suggested to be related to the binding of ^{65}Cu to strong organic ligands in the aqueous phase (Vance et al., 2008, 2016). It is possible that the preferential adsorption of ^{63}Cu onto SPM and oxic soils may also be related to adsorption onto birnessite (Ijichi et al., 2018; Little et al., 2014b; Sherman and Little, 2020) or clay minerals, such as kaolinite (Li et al., 2015). Interestingly, it was originally hypothesized that the adsorption of Cu onto birnessite should result in the enrichment of ^{65}Cu because of the change in the coordination environment of Cu^{2+} and the shortening of bond lengths between aqueous and adsorbed Cu^{2+} (Little et al., 2014a). However, Cu adsorbed to the Fe-Mn oxide fraction of Fe-Mn crusts is enriched in ^{63}Cu relative to seawater ($\Delta^{65}Cu_{Fe\text{-}Mn\ oxides\ -\ Seawater} = -0.60$ to −0.40‰) (Little et al., 2014b). Recent laboratory experiments also demonstrated that ^{63}Cu is preferentially adsorbed onto birnessite (Ijichi et al., 2018), and this was confirmed computationally using ab initio calculations (Sherman and Little, 2020).

Organic complexes play an important role in Cu binding in the organic matter and aqueous phase of soils, with soil organic matter being observed to preferentially adsorb ^{65}Cu (Bigalke et al., 2010a, 2010b, 2010c). This is likely related to the preferential complexation of ^{65}Cu with humic acids, which are an important component of humus, the major organic fraction in soil (Bigalke et al., 2010c). Further, Ryan et al. (2014) showed that ^{65}Cu is enriched over ^{63}Cu during complexation to a range of soluble organic ligands relative to inorganic aqueous species. Conversely, significant enrichment of ^{63}Cu has been observed on the cell surface of the soil bacterium, *P. aureofaciens*, at an ultra-acidic pH of between 1.8 and 3.5. However, at a more typical soil pH of between 4 and 7, both reversible short-term adsorption and assimilation during cell growth produced isotopic shifts that were comparable to the measurement uncertainty (Pokrovsky et al., 2008).

Compared to Zn, for which an abundance of data on isotope fractionation during adsorption is available (birnessite, pyrolusite, ferrihydrite, goethite, hematite, gibbsite, corundum, γ-Al_2O_3, quartz, amorphous SiO_2,

diatoms, bacteria, humic acids, kaolinite, calcite), little data is available for the adsorption of Cu (Komárek et al., 2021). This complicates the use of the Cu ratio as a vector in mineral exploration and as a tracer of origin, transport, and fate of metal contaminants in the environment. Along with kaolinite, montmorillonite and illite are the most common clay minerals in soil systems and play an important role in metal adsorption (Du et al., 1997). Copper isotope fractionation during adsorption onto the surfaces of these clay minerals should be investigated. Hematite, chlorite, vermiculite, and quartz, should also be prioritized in decreasing order of their importance to the adsorption of Cu in soils (González-Costa et al., 2017) to enhance our understanding of Cu isotope fractionation mechanisms in the natural surface environment.

4.3. Biologically-mediated reactions

In biologically-mediated reactions where no equilibrium is established, compounds containing the lighter isotope, ^{63}Cu, have lower activation energies, allowing them to react faster (Mathur et al., 2005; Pokrovsky et al., 2008; Zhu et al., 2002). Zhu et al. (2002) identified that the incorporation of Cu in proteins (metallothioneins and SOD) from bacteria and yeast cells results in the preferential uptake of ^{63}Cu, with the $\delta^{65}Cu$ of cells being as much as ~1.7‰ lower than in the source solution. There is further Cu isotope fractionation between different amino acids and proteins due to the tendency of the heavier isotope, ^{65}Cu, to concentrate in compounds when binding with more electronegative ligands (Albarède et al., 2011; Télouk et al., 2015). For example, Cu bound to histidine (Cu-N bonds), as in superoxide dismutase (SOD) is expected to be more concentrated in ^{65}Cu than in proteins in which Cu bound to the cysteine-rich protein, metallothionein (Cu-S bonds) (Fujii et al., 2014; Larner et al., 2019; Télouk et al., 2015). Together with oxidation state, ligand electronegativity plays a prominent role in determining Cu isotope fractionation patterns in different blood compartments, organs, and cell organelles (Albarède et al., 2017).

Bacterial reduction is also an important control and can result in a large degree of Cu isotope fractionation. Navarrete et al. (2011a) found that lab strains and natural consortia used to study Cu isotope fractionation during intracellular incorporation preferentially incorporated ^{63}Cu with a $\Delta^{65}Cu_{\text{Solution – Solid}}$ of 1.0 to 4.4‰. This was proposed to be a result of active cellular transport and regulation, including the reduction of Cu^{2+} to Cu^{+}, and these potential fractionation mechanisms are likely also occurring in fungi, plants, and higher organisms due to their shared intracellular structures and mechanisms (Navarrete et al., 2011a).

Metals are primarily accumulated in plants through root and foliar uptake (Shahid et al., 2017). Copper isotope fractionation during Cu uptake has been documented by a number of groups (Blotevogel et al., 2019, 2022; Jouvin et al., 2012; Li et al., 2016, 2020; Navarrete et al., 2011b; Ryan et al., 2013; Weinstein et al., 2011; Zheng et al., 2005; Zhu et al., 2010), and a recent review summarizes stable isotope fractionation of metals (including Cu) and metalloids in plants (Wiggenhauser et al., 2022). Zheng et al. (2005) and (Li et al., 2016) propose the reduction of Cu^{2+} by FRO-type reductase at the soil solution-root interface as an important Cu isotope fractionation mechanism during Cu uptake. From the soil solution, Cu^{+} is taken up into the plant and Cu^{0} is adsorbed onto the root surface (Li et al., 2016). This results in an overall enrichment of ^{63}Cu in the plant relative to soil and soil solution, although further isotope fractionation occurs after uptake as Cu is distributed throughout plant organs and tissues (Wiggenhauser et al., 2022). For instance, oxidation at the root-xylem interface leads to the enrichment of ^{65}Cu in aboveground tissues relative to root tissue (Li et al., 2016), although this appears to be species-dependent (Wiggenhauser et al., 2022).

5. Exploration geochemistry

5.1. Copper isotope ratio variations related to ore deposits

Ore deposits are the most important source of Cu and metal production globally accounts for the majority (~70%) of Cu emitted to the atmosphere (Rauch and Pacyna, 2009). As such, ore deposits have been the subject of a large body of research undertaken on investigating Cu stable isotope fractionation. This is due to the ability of the Cu isotope ratio to trace the origin of Cu from the point of collection in the environment. Research has been conducted on volcanogenic massive sulfide (VMS) deposits, including Kalatag (Deng et al., 2019), Alexandrinka (Mason et al., 2005), Las Cruces (Miguélez et al., 2019), the Pontides province in Turkey (Housh and Çiftçi, 2008), and Japanese Besshi type deposits (Ikehata et al., 2011), skarn deposits (Larson et al., 2003; Su et al., 2018), and magmatic Ni-Cu deposits, such as Arylakh in Noril'sk Province (Malitch et al., 2014), and Tulaergen in China (Zhao et al., 2017). Limited work has also been undertaken on sediment-hosted Cu deposits (Asael et al., 2007). However, by far the majority of work has focused on porphyry Cu deposits, which form very large accumulations of disseminated Cu (Richards, 2021). The mineralogical composition of these deposits commonly makes the elements accumulated within them amenable to remobilisation after formation, which can produce economically significant accumulations of supergene Cu minerals. In terms of mineral exploration, the main focus is on the use of $\delta^{65}Cu$ to detect concealed ore deposits in areas of depleted Cu concentration (leached or highly weathered) or post-mineral cover accumulation.

The upper exposed portions of porphyry deposits commonly undergo weathering, oxidation, and element recycling, resulting in a classic supergene profile of leached cap, secondary Cu oxide, sulfate, and chloride mineralization, and supergene enriched Cu sulfide zone, all overlying hypogene Cu sulfide mineralization (Sillitoe, 2010). In particular, the oxidation of primary sulfide minerals results in leaching (Kidder et al., 2021, 2022) and the release of Cu, which migrates in aqueous solution and precipitates due to reducing conditions below the water table (Boyle, 2003; Lichtner and Biino, 1992). The precipitation of supergene minerals such as chalcocite commonly forms a distinct zone or blanket, which is termed the supergene sulfide enrichment zone (Reich et al., 2009). Finally, the original primary sulfide minerals (unweathered) are referred to as the hypogene zone (Reich et al., 2009).

The effectiveness of $\delta^{65}Cu$ values to differentiate these three horizons has been demonstrated in a number of studies. Combined data reveal that the $\delta^{65}Cu$ values of hypogene minerals range from −2.56 to 7.24‰ (median 0.18‰), supergene minerals range from −16.49 to 8.30‰ (median 0.92‰), and leached cap/oxide minerals range from −14.64 to 9.98‰ (median −0.60‰) (Braxton and Mathur, 2011; Graham et al., 2004; Li et al., 2010; Mathur et al., 2009, 2010, 2012, 2013; Mirnejad et al., 2010; Palacios et al., 2011; Wu et al., 2017). Large variations in Cu stable isotope ratios ($\delta^{65}Cu$ ranging from −16.49 to 9.98‰) are reported in Mathur et al. (2010), Mathur et al. (2009), and Mirnejad et al. (2010), but generally, the range of $\delta^{65}Cu$ values for hypogene, supergene, and leached cap/oxide minerals is more limited. The $\delta^{65}Cu$ values of primary sulfide minerals (chalcopyrite and bornite) typically range from −0.1 to 0.5‰ (Cooke et al., 2014). Secondary ore zones from the Spence deposit (Chile) show significant departures from the $\delta^{65}Cu$ of primary sulfide minerals (0.29 to 0.34‰), with supergene chalcocite ranging from 3.91 to 3.95‰ and chrysocolla ranging from 1.28 to 1.37‰ (Palacios et al., 2011). Atacamite, which formed last by interaction with hypersaline fluids, represents a significant reversal with values ranging from −6.77 to −5.72‰ (Palacios et al., 2011). Braxton and Mathur (2011) identified a trend of decreasing $\delta^{65}Cu$ values from an enriched source zone (>3‰) at the Bayugo porphyry (Philippines) to distal exotic mineralization (<1‰) and attributed it to Rayleigh-type fractionation with repeated leaching and precipitation. Like in other studies, mineralized zones at Bayugo are isotopically distinct, with the $\delta^{65}Cu$ value for the original primary hypogene mineralization (−0.6 to 1.0‰) being much lower than those for the enriched secondary mineralization in the supergene zone (2.23 to 2.56‰) and leached cap Fe oxide minerals (1.8 to 2.7‰). At the Cañariaco Norte porphyry deposit (Peru), $\delta^{65}Cu$ values identify possible pre-existing supergene mineralization or potential for an undiscovered zone of exotic mineralization laterally away (Mathur et al., 2012). Iron oxide minerals from the leached cap display very low $\delta^{65}Cu$ values (−8.42 to −2.29‰) compared to the average $\delta^{65}Cu$ values for hypogene mineralization of 0.18 ± 0.32‰, and this is

suggested to result from intense oxidative weathering (Mathur et al., 2012). Li et al. (2010) demonstrated the use of δ^{65}Cu values as an exploration vectoring tool, with the recognition of lateral zonation in the Northparkes (Cu-Au) porphyry (Australia). Variability in excess of 1‰ (ranging from −1.67 to 0.91‰) in sulfide samples was reported, with δ^{65}Cu values decreasing from 0.29 ± 0.56‰ (n = 20) in low-grade peripheral alteration zones to −0.25 ± 0.36‰ (n = 30) at the margins of mineralized zones (Li et al., 2010).

5.2. Exploration hydrogeochemistry

Low-temperature, post-depositional (secondary) dispersion of Cu can produce geographically-large Cu isotope ratio footprints in environments where Cu concentrations are relatively low or similar to background and otherwise do not reveal proximal mineralization (Kidder et al., 2021, 2022; Mathur et al., 2013; Su et al., 2018). These footprints have been identified in low salinity and neutral groundwaters, leached caps of mineral deposits, and areas of deep post-mineral cover where the upward mobility of Cu is limited. Despite this, there has been very limited application of the δ^{65}Cu value in exploration hydrogeochemistry.

Surface and groundwaters that interact with undisturbed deposits commonly have several orders of magnitude lower concentration of trace metals compared to water impacted by acid rock drainage (ARD)-related processes (Ficklin et al., 1992; Goodfellow, 2007; Plumlee et al., 1999). A key case study is the Pebble porphyry deposit (Alaska), where the oxidative dissolution of chalcopyrite in the orebody is accompanied by a high degree of Cu isotope fractionation in the shallow groundwater seeps and streams proximal to the orebody that are relatively enriched in ^{65}Cu (Mathur et al., 2013). Groundwaters proximal to the Picaron porphyry prospect (Chile) and the Kitumba Fe-oxide-Cu-gold (IOCG) deposit (Zambia), as well as other deposit types (massive sulfide, skarn, and epithermal), are also relatively enriched in ^{65}Cu (Kidder et al., 2021, 2022; Mathur et al., 2013; Su et al., 2018). Mathur et al. (2013) reported a decreasing trend for the δ^{65}Cu value of dissolved Cu in shallow groundwater seeps and streams sampled from proximal to Pebble to more distal sites. Similarly, groundwater proximal to mineralization at Picaron has δ^{65}Cu values that are estimated to be up to ~2.3‰ higher than mineralization and decrease downgradient from the mineralization (Kidder et al., 2021). Downgradient Cu stable isotope fractionation has been attributed to adsorption onto Fe oxide minerals (Mathur et al., 2014; Su et al., 2018) and Fe-Mn oxide minerals (Kidder et al., 2021), but this is most likely related to preferential adsorption of ^{65}Cu to metal oxyhydroxide minerals (Balistrieri et al., 2008; Pokrovsky et al., 2008), a ubiquitous phase for sequestering metals and other elements in soil and sediment, or it is caused by mixing with other Cu sources (Kidder et al., 2021).

6. Tracing anthropogenic sources of Cu

Copper is a vital micronutrient that facilitates numerous biological processes in organisms (Weinstein et al., 2011), but it can be toxic at high concentrations (Yruela, 2005). This has driven interest in the use of the Cu isotope ratio for identifying sources of anthropogenic Cu contamination. Anthropogenic materials, such as cement, road dust, motor vehicle products, antifouling paint, Cu pesticides, pig slurry, flotation tailings, slag, urban aerosols, and particles originating from smelting and flue gas cleaning processes are generally characterized by δ^{65}Cu values that are higher than geological materials, including upper continental crust (0.07 ± 0.10‰), uncontaminated sedimentary materials from estuaries (−0.04 ± 0.18‰), and SPM from rivers, wetlands, and estuaries (−1.02 to 0.09‰, −0.31 ± 0.10‰ mean) (Araújo et al., 2019a, 2021b; Babcsányi et al., 2016; Blotevogel et al., 2018; Briant, 2014; Dong et al., 2017; El Azzi et al., 2013; Fekiacova et al., 2015; Gelly et al., 2019; Gonzalez et al., 2016; Kříbek et al., 2018; Liu et al., 2015; Savage et al., 2015; Schleicher et al., 2020; Souto-Oliveira et al., 2018, 2019; Takano et al., 2020; Wang et al., 2017).

Traffic-related Cu sources, including PM_{10} (inhalable particles with diameters of <10 μm) road tunnel dust, road dust, road furniture, brakes, and tires have δ^{65}Cu ranging from −0.18 to 0.71‰ (median = 0.34‰), with road paint and pavement having values over 0.55‰ (Dong et al., 2017; Schleicher et al., 2020). The δ^{65}Cu values of urban aerosols from Barcelona (Spain), London (United Kingdom), Metz (France), Zaragoza (Spain), and São Paolo (Brazil) range from −0.42 to 0.98‰ (Schleicher et al., 2020). The Cu isotopic composition of aerosols at the Dongsha Atoll in the northern South China Sea are comparable, with δ^{65}Cu values ranging from −0.13 to 0.83‰ in $PM_{2.5–10}$, and from −0.33 to 0.37‰ in $PM_{2.5}$, and this is speculated to be related to Cu emissions from local anthropogenic activities (Takano et al., 2020). The δ^{65}Cu value of cement in São Paolo ranges from 0.10 to 0.61‰, and is in agreement with the Cu isotopic signatures of raw materials used for cement production (Souto-Oliveira et al., 2018, 2019).

Smelter emissions are another common source of Cu, which is typically distributed as airborne particulates that become incorporated in soils. It is generally accepted that Cu is not fractionated during the smelting processes as Cu is only volatile above 2595 °C, higher than common smelting temperatures (Gale et al., 1999; Gelly et al., 2019). Therefore, the δ^{65}Cu values of emissions from smelters generally reflect the original composition of processed ores, although Cu isotope fractionation has been reported during transit (Bigalke et al., 2011; Gelly et al., 2019; Mattielli et al., 2006). At the Escalette smelter (France), chimney coatings have a δ^{65}Cu value of −0.46 ± 0.01‰ at the base that increases to −0.22 ± 0.04‰ at the top, suggesting that the chimney coatings retain ^{63}Cu and the vapour phase is relatively enriched in ^{65}Cu (Gelly et al., 2019). The δ^{65}Cu value for slag ranges from −1.70 to 0.55‰ and particles originating from smelting and flue gas cleaning processes show δ^{65}Cu values ranging from 0.15 to 0.49‰, whereas the δ^{65}Cu values for flotation tailings range from 0.95 to 1.1‰ (Araújo et al., 2021b; Briant, 2014; Gelly et al., 2019; Kříbek et al., 2018; Souto-Oliveira et al., 2018). Slag and smelter feed from north-east Norway have relatively low δ^{65}Cu values of −1.67 ± 0.04‰ and − 1.68 ± 0.15‰, respectively, but this is enriched in ^{65}Cu relative to the remarkably depleted bedrock (δ^{65}Cu values ranging from −3.52 ± 0.16‰ to −3.04 ± 0.32‰) from which they are likely derived (Šillerová et al., 2017). Surficial (oxidized) tailings in the tropical mining region of Taxco, Guerrero (southern Mexico) have δ^{65}Cu values ranging from −1.91 to 0.91‰, with a mean of −0.32‰ (Dótor-Almazán et al., 2017). Pérez Rodríguez et al. (2013) reported a δ^{65}Cu value of 1.32 ± 0.03‰ in unoxidized tailings at the Laver mine (Sweden). This is in contrast to a δ^{65}Cu value of around 0‰ for oxidized tailings and a δ^{65}Cu value as low as −4.34 ± 0.02‰ at the redox-boundary zone. The depletion of ^{65}Cu in oxidized tailings is likely due to the oxidation of primary sulfide minerals that results in the enrichment of ^{65}Cu in Cu^{2+} in the aqueous phase. The enrichment of ^{63}Cu in the redox-boundary zone is likely due to the preferential adsorption of ^{65}Cu onto Fe-oxyhydroxide minerals during fluid percolation and the precipitation of the secondary Cu mineral, covellite. Conversely, at Chañaral Bay (Chile), the biotic fractionation of Cu isotopes by microorganisms is invoked as a mechanism to explain lower δ^{65}Cu values at the base of the mine tailings (0.42‰) compared to the surface (0.92‰) (Roebbert et al., 2018).

Efforts are being made to trace agricultural contaminants, which can end up in microorganisms, wildlife, humans, soils, SPM, river water, and ocean water. In the case of pesticides, δ^{65}Cu values vary significantly (ranging from −0.49 to 0.91‰), depending on the Cu speciation and manufacturing date, which complicates their tracing (Babcsányi et al., 2016; Blotevogel et al., 2018; El Azzi et al., 2013). Pig slurry also has variable δ^{65}Cu values, but it is consistently enriched in ^{65}Cu (0.12 and 0.52‰) (Fekiacova et al., 2015).

6.1. Soils and surficial sediments

The determination of both Cu concentrations and the Cu isotope ratio in soils is used in environmental and mineral exploration studies as a vector towards the source (anthropogenic or ore deposit from which the Cu was dispersed). However, soil Cu isotopic compositions vary independently

from Cu concentrations and correlate with organic matter, making them more sensitive indictors of changes in soil chemistry (Fekiacova et al., 2015). Surface soils sampled proximal to smelter, mining, industrial, and agricultural operations commonly display δ^{65}Cu values that reflect anthropogenic Cu input, with decreasing influence at depth. This has most commonly presented as a decrease in δ^{65}Cu values with increasing soil profile depth, but this can depend on the soil horizon sampled (Bigalke et al., 2010a; Fekiacova et al., 2015; Kusonwiriyawong et al., 2017; Mihaljevič et al., 2018, 2019; Wang et al., 2022a).

In a review of Cu isotopic compositions in polluted and unpolluted soils, Fekiacova et al. (2015) reported that polluted soils (defined in articles as those where pollution is explicitly mentioned or where soils have anomalous metal concentrations (Baize, 1997)) have δ^{65}Cu values that are significantly enriched in ^{65}Cu (~0.2‰) compared to unpolluted soils (~0‰). It is possible that this general tendency of polluted soils to be enriched in ^{65}Cu is linked to the typically high δ^{65}Cu of anthropogenic Cu sources. Indeed, the δ^{65}Cu of road-deposited sediment in the Shihwa National Industrial Complex in Ansan (South Korea) ranges from −0.12 to 0.94‰ (Jeong and Ra, 2021). This trend is also observed around the city of Luleå (Sweden), which is industrialized with steelworks and harbours (Pallavicini et al., 2018). In the city (samples taken within 5 km of local industries), soils are relatively enriched in ^{65}Cu compared to suburban soils (samples taken approximately 10 km from local industries) (Pallavicini et al., 2018). However, there are exceptions to this tendency. In surface horizon soils and floodplain sediments near wine-producing areas, low δ^{65}Cu values (−0.37 to −0.14‰) reflect the spraying of the Bordeaux mixture ($Cu(OH)_2$ + $CuSO_4$, −0.34 ± 0.08‰), a fungicide that is sprayed in vineyards, fruit farms, and gardens to control vine downy mildew (Chen et al., 2008; El Azzi et al., 2013; Petit et al., 2013). However, it is difficult to make generalizations about the δ^{65}Cu trends of pesticide-contaminated soils because the δ^{65}Cu value of pesticides varies greatly (−0.49 to 0.91‰) (Babcsányi et al., 2016; Blotevogel et al., 2018; El Azzi et al., 2013).

At the Kombat mine site (Namibia), the variation of δ^{65}Cu with depth is attributed to different source endmembers, with near-surface soils reflecting dust-blown tailings Cu and deeper soil horizons reflecting bedrock materials (Mihaljevič et al., 2019). Adsorption may also play a role as soil water descends through the soil profile, with adsorption onto metal oxyhydroxide minerals and organic matter favouring the retention of the heavier ^{65}Cu (Moynier et al., 2017). The favouring of ^{65}Cu during complexation with soil organic matter is further demonstrated in a study that assessed the severity of soil pollution and bioavailability of Cu in soils at various distances from a Ni refinery (Lower Swansea Valley, United Kingdom), with soil organic matter being enriched in ^{65}Cu compared to dissolved bioavailable Cu ($\Delta^{65}Cu_{Organic\ -\ Bioavailable}$ = 0.12 ± 0.13‰) (Schilling et al., 2021). Soil metal contents are predominantly associated with organic matter, which reduces their bioavailability, so the Cu isotope ratio may be used as a proxy for metal bioavailability and shows potential for tracing the fate and mobility of Cu in soils (Schilling et al., 2021). A Cu isotopic signature from the oxidative weathering of skarn-derived Cu sulfide minerals in the historic mining area of Tongling (China) could be identified in the upper portions of soils (5 to 100 cm) within 1 km of the tailings (Su et al., 2018). Soil samples collected from the Tsumeb mining district (Namibia) display higher δ^{65}Cu values (0.13 to 0.76‰) compared to soils from an uncontaminated area (δ^{65}Cu = −0.01 to 0.14‰), allowing for the identification of contaminated sites (Kříbek et al., 2018). This was suggested to reflect the Cu isotopic composition of old flotation tailings (δ^{65}Cu = 0.95 to 1.1‰), slag (0.11 to 0.55‰), and particles originating from the smelting and flue gas cleaning processes (0.15 to 0.49‰). Conversely, both proximal and distal to the Nkana Cu smelter in the Zambian Copper Belt (ZCB), the δ^{65}Cu value of the surface soil (−0.44 to −0.40‰) is similar to that of the concentrates processed in the smelter (−0.75 to −0.45‰), with both locations appearing to be affected by Cu ore dust (Mihaljevič et al., 2018). The δ^{65}Cu values of organic matter-rich topsoil (−2.40 ± 0.04‰ to −0.43 ± 0.08‰) near a smelter in northeast Norway appear to reflect a combination of the local bedrock (−3.52 ± 0.16‰ and −3.04 ± 0.32‰), slag and smelter feed (−1.68 ± 0.15‰ and −1.68 ± 0.04‰, respectively), and the preferential adsorption of ^{65}Cu onto organic matter (Moynier et al., 2017; Šillerová et al., 2017).

Despite the general tendency of anthropogenic Cu sources to have higher δ^{65}Cu values than geological sources (~0‰), it can be difficult to define a specific δ^{65}Cu value range for the fingerprinting of Cu derived from mining-related activities, as the δ^{65}Cu values of the original local geological materials and their products can vary considerably (Novak et al., 2016; Šillerová et al., 2017). Given the same applies to most other materials, the δ^{65}Cu values of potential natural and anthropogenic Cu sources in a given study area must be determined to enable their fingerprinting.

6.2. Vegetation

It was previously proposed that due to the preferential incorporation of ^{63}Cu by bacterial species, fungi, plants, and higher organisms, the Cu isotope ratio may serve as a marker for terrestrial biological activity (Navarrete et al., 2011a). However, this proposal is challenged by more recent work that demonstrates that an isotopically light Cu signature is not unique to biological uptake, with ^{63}Cu concentrating during reductive precipitation of Cu-bearing minerals (Ehrlich et al., 2004; Pękala et al., 2011; Qi et al., 2019) and preferentially adsorbing onto SPM, oxic soils, birnessite, and kaolinite (Ijichi et al., 2018; Li et al., 2015; Sherman and Little, 2020; Vance et al., 2008, 2016; Wang et al., 2017). Fortunately, the Cu uptake patterns of organisms can be leveraged in other ways, and there is a growing body of work that demonstrates that Cu isotopic analysis of vegetation can be a powerful tool for tracing anthropogenic sources of Cu.

Vegetation (including trees and their various organs) reflects the geochemistry of the substrate and represents an advantageous sampling medium for exploration and environmental geochemistry because vegetation occurs globally in most environments and root systems are commonly vast, resulting in the collection of mobile elements over larger areas and depths than soils, which rather represent a point sample (Kyser et al., 2015). Determination of the Cu isotope ratio in plants is just beginning to play a role in tracing the pathways of metal migration from contaminated sites, and in order to effectively employ this approach, several important variables must be controlled for when sampling vegetation as they can influence isotopic compositions. These include selection of species (influences Cu uptake), compartment sampled (root, stem, leaves, flowers, etc.), and height of the plant growth at which they are sampled (Jouvin et al., 2012; Li et al., 2016; Navarrete et al., 2011b; Ryan et al., 2013; Weinstein et al., 2011; Zheng et al., 2005; Zhu et al., 2010).

Grass specimens collected from the Tsumeb mining district (Namibia) display higher δ^{65}Cu values (0.15 to 0.64‰) compared to grasses from an uncontaminated area (δ^{65}Cu = −0.17 to 0.03‰) (Kříbek et al., 2018). As for Tsumeb soils, this likely reflects the Cu isotopic composition of mineral processing-related materials. In addition to the analysis of soils, Mihaljevič et al. (2018) reported the δ^{65}Cu values for tree cores from pines in areas impacted by Cu ore dust around a Cu smelter in the ZCB. Tree rings proximal to contaminated sites display δ^{65}Cu ranges similar to the values obtained for contaminated soils and processed ore (−0.88 to −0.31‰), compared to lower values (−2.22 to −0.76‰) at the less contaminated site. These patterns were suggested to be the product of the interception of Cu dust particles rather than uptake by tree roots (Mihaljevič et al., 2018). The particular advantage of tree cores as a sampling medium is that they reflect a chronology of their chemical environment and can serve as a temporally-resolved record of anthropogenic activity, with older trees even having the potential to provide a reliable record of pre-global industrialization conditions (Kyser et al., 2015; Schmidt et al., 2017). However, to the best of our knowledge, this potential to identify anthropogenic input over time has not been taken advantage of with Cu isotopic analysis and represents a promising future research opportunity.

6.3. Aquatic settings

Vance et al. (2008) presented an extensive dataset of δ^{65}Cu values for rivers worldwide and constrained a δ^{65}Cu range for dissolved Cu of 0.02

to 1.45‰, with a discharge-weighted average of 0.68‰. Similarly, the best estimate to date for the Cu isotopic composition of seawater is about 0.65‰ (Little et al., 2018). In contrast, a complementary light Cu isotopic pool is present in SPM from aquatic environments (rivers, wetlands, estuaries; δ^{65}Cu = −1.02 to 0.09‰, −0.31 ± 0.10‰ mean) and uncontaminated sedimentary materials from estuaries (−0.04 ± 0.18‰) (Araújo et al., 2019a; Wang et al., 2017). The heavier Cu isotopic composition of dissolved Cu from river and seawater is most likely due to the enrichment of ^{65}Cu during organic inner sphere complexation of Cu, which is the dominant form of Cu^{2+} binding in the dissolved phase of natural waters (Moynier et al., 2017), whereas the negative δ^{65}Cu values of solids relative to the upper continental crust (0.07 ± 0.10‰) are potentially linked to the preferential adsorption of ^{63}Cu onto Mn oxide minerals and clays, as well as microbial uptake (likely involving a redox conversion) (Ijichi et al., 2018; Li et al., 2015; Navarrete et al., 2011a; Pokrovsky et al., 2008; Sherman and Little, 2020; Takano et al., 2021; Vance et al., 2008, 2016).

Recent studies demonstrate Cu isotope fractionation in stream water, river water, and groundwater around hydrothermal mineral deposits that is likely related to the oxidative dissolution of Cu sulfide minerals, yielding δ^{65}Cu values that are significantly higher (up to ~2‰) than the original source compositions at the onset of ARD (Balistrieri et al., 2008; Borrok et al., 2008; Fernandez and Borrok, 2009; Kimball et al., 2009; Masbou et al., 2020; Pontér et al., 2021; Viers et al., 2018). The oxidative dissolution of Cu sulfide minerals can even impact the Cu isotopic composition of larger systems, such as the Yangtze River (China) (Wang et al., 2020b). The Yangtze River and its tributaries display much higher dissolved δ^{65}Cu values (0.59 to 1.65‰ and 0.48 to 1.20‰, respectively) compared to the discharge-weighted average of 0.68‰ for rivers worldwide, reflecting, in part, the presence of numerous Cu sulfide deposits (Vance et al., 2008; Wang et al., 2020b).

Despite waters being the primary means of Cu dispersion in ARD-affected areas around mined or unmined mineralization, and evidence of unanimously elevated δ^{65}Cu values in waters that have interacted with Cu sulfide minerals, there are very few studies that seek to trace Cu sources and dispersion pathways using Cu isotopic analysis. Masbou et al. (2020) demonstrated the potential of the δ^{65}Cu value of water from the Meca River (Spain) to trace Cu contamination from the Tharsis Mine in the Iberian Pyrite Belt (IPB, Spain), with the δ^{65}Cu values for upstream samples varying from −0.47 to −0.08‰ and downstream samples varying from −0.63 to 0.31‰ (Masbou et al., 2020). Higher δ^{65}Cu values upstream were attributed to the oxidative dissolution of primary sulfide minerals, whereas downstream, similar to what is reported in Kidder et al. (2021), Mathur et al. (2013, 2014), and Su et al. (2018), the decrease in δ^{65}Cu is most likely related to the preferential adsorption of ^{65}Cu onto metal oxyhydroxide minerals (Balistrieri et al., 2008; Pokrovsky et al., 2008), or mixing with other Cu sources (Kidder et al., 2021). Similarly, Viers et al. (2018) reported δ^{65}Cu values in river water proximal to ARD-producing deposits in the IPB that are higher than in background mining waters, percolating shallow groundwater, and lake water. This likely results from the oxidative dissolution of Cu sulfide minerals. However, contrary to observations by Masbou et al. (2020), the decrease in dissolved Cu is accompanied by an increase in δ^{65}Cu values, which they suggest to be the result of Cu-bearing secondary mineral precipitation and groundwater input (Viers et al., 2018). Similar results were reported near the Rönnskär sulfide ore smelter (Sweden) (Pontér et al., 2021). Here, a significant decrease in dissolved Cu concentrations was accompanied by a trend of increasing δ^{65}Cu values distally from dust deposit leachate-to-dust deposit well water-to-groundwater (Pontér et al., 2021). Importantly, although these studies were conducted with the goal of tracing environmental pollution, this same study design and data (as shown earlier) can potentially help guide exploration geochemists in search of mineral deposits (Kidder et al., 2021, 2022; Mathur et al., 2013, 2014; Su et al., 2018).

Recently, researchers have demonstrated the potential of δ^{65}Cu to trace the source of industrial and agricultural activities proximal to lake, ocean, and river systems (Petit et al., 2013; Takano et al., 2020; Thapalia et al., 2010; Wang et al., 2020b; Zeng and Han, 2020). For example, Cu isotopic analysis of a sediment core from Lake Ballinger near Seattle (Washington, USA) has been used to identify the sources and timing of metal deposition (Thapalia et al., 2010). The δ^{65}Cu values vary by 0.29‰ over the 500-year core record, with the pre-smelter period (~1450 to 1900) characterized by a δ^{65}Cu of 0.77 ± 0.06‰, which increased to 0.94 ± 0.10‰ during the period of smelter operation (1900 to 1985), before decreasing back to 0.82 ± 0.12‰ during the post-smelting/stable urban land use period (post-1985) (Thapalia et al., 2010). Petit et al. (2013) measured δ^{65}Cu values for dissolved Cu in creeks draining vineyards that are relatively enriched in ^{63}Cu, indicating the influence of anthropogenic contamination from the spraying of Cu sulfate fungicides. Araújo et al. (2019a) used surface sediments in Toulon Bay (France) to study metal contamination induced by past and recent naval activities. Elevated Cu concentrations and negative δ^{65}Cu values compared to uncontaminated areas were attributed to the mixing of ancient and modern anthropogenic sources of Cu by the reworking of sediments (Araújo et al., 2019a). An interesting application of the Cu isotope ratio that has emerged is the calculation of the relative contribution of different sources of Cu in SPM. Based on Cu isotopic compositions (δ^{65}Cu ranging from 0.04 to 0.50‰ with a mean of 0.17‰) and mass balance equations for SPM from the Zhujiang River (China), 76.4% of particulate Cu in the Zhujiang River is sourced from rock weathering, whereas urban sludge and smelting tailings contribute 15.4% and 8.2%, respectively (Zeng and Han, 2020). In support of this method for determining the relative contribution of different sources to Cu found in SPM, the initial isotopic composition of Cu source material may be preserved during the mixing of two chemically distinct rivers (Guinoiseau et al., 2018). Most recently, it was demonstrated that the contaminant-tracing potential of the Cu isotope ratio is not limited to water, sediment, and SPM from lakes, oceans, streams, and rivers, as δ^{65}Cu and Sb/Cu values indicate that road dust (and to a lesser extent fossil fuel combustion) is the dominant source of Cu in rain (δ^{65}Cu of −0.23 to 0.87‰), snow (δ^{65}Cu of 0.00 to 0.57‰), and rime (δ^{65}Cu of 0.12 to 0.67‰) samples from Uji City and Mt. Kajigamori (Japan) (Takano et al., 2021). This is in contrast to rainwater collected from rural and urban regions of Japan that has δ^{65}Cu values ranging from −0.12 to 0.03‰ (Takano et al., 2014), and snow (−1.07 to −0.24‰, −0.46 ± 0.15‰ mean) which is affected by smelter emissions derived from smelter feed possessing a mean δ^{65}Cu value of −1.68 ± 0.15‰ (Šillerová et al., 2017).

6.4. Cu stable isotopes as a biomonitoring tool

The potential of Cu isotopic analysis as a biomonitoring tool is just beginning to be explored, with the δ^{65}Cu value of bivalve molluscs showing promise as monitors of anthropogenic Cu contamination in coastal and marine ecosystems (Araújo et al., 2021a, 2021b, 2022). Bivalve molluscs are filter feeders that bioaccumulate trace metals and their tissues can serve as monitors of metal bioavailability over time. *Crassostrea gigas* (oyster) and *Mytilus edulis* (mussel) that were monitored in a French coastal site contaminated by diffuse anthropogenic Cu sources show δ^{65}Cu values that increase in tandem with Cu bioavailability, reflecting the ^{65}Cu-enriched signature typical of mostly anthropogenic Cu inputs (Araújo et al., 2021b; Briant, 2014; Kříbek et al., 2018; Souto-Oliveira et al., 2018). *Crassostrea gigas* further displayed its use as a biomonitoring organism in a study that transplanted 18-month old oysters from a relatively pristine area to Arcachon Bay, France which is experiencing increasing Cu contamination (Araújo et al., 2021a). After 12 months in their new location, the oysters' bodily Cu burdens increased and showed a gradient of increasingly positive δ^{65}Cu values with proximity to unknown continental Cu source(s), which taken together indicates a dominantly anthropogenic continental Cu source (Araújo et al., 2021a).

7. Isotope metallomics

Copper is a trace element that is essential for the functioning of organs and metabolic processes in humans (Uauy et al., 1998). Copper makes its way into the body primarily through the consumption of foods, but

drinking water accounts for about 6 to 13% of the average daily intake (Fitzgerald, 1998; Gaetke and Chow, 2003). Copper also enters the body through inhalation of air particulates derived from natural sources, such as windblown dust, volcanic particulates, and forest fires, but also from anthropogenic sources, including Cu smelters, iron and steel production, and incinerators (Gaetke and Chow, 2003). Once in the body, the majority of Cu (occurring mostly as Cu^{2+}) absorption occurs in the small intestine, with a smaller amount absorbed in the stomach (Gaetke and Chow, 2003; Turnlund et al., 1997). Although an essential nutrient, excessive levels of Cu can accumulate through ingestion of contaminated food and drink, occupational hazards, or environmental contamination, commonly to ill effect (Kelvin et al., submitted). Primarily, chronic Cu toxicity affects the liver because it is the first site of Cu deposition after entering the blood following absorption (Gaetke and Chow, 2003). This toxicity is typically manifested by the development of liver cirrhosis, and some progress has been made towards improving diagnosis and prognosis (Costas-Rodríguez et al., 2015; Lauwens et al., 2018). There may be further potential in this area for not only improving the ability to diagnose and prognose liver cirrhosis, but also tracing anthropogenic sources of excess Cu.

Natural errors of Cu metabolism can also cause deviations from typical Cu concentrations and isotope ratios in different compartments within the body. There is a growing research base utilizing δ^{65}Cu to study metal homeostasis and its disruption in the human body. Other elements, such as Fe, Zn, Mg, and Ca have also been used, but the majority of studies thus far have investigated Cu. There are several possible reasons for this. Compared to Zn, Cu likely has a greater specificity for biological processes due to being 10 to 60 times less abundant in the body than Zn (Albarède et al., 2017; Gropper and Smith, 2012). Additionally, Cu isotope fractionation tends to be more intense and driven by a redox shift between Cu^{+} and Cu^{2+}, whereas Zn is not redox-sensitive. Unlike for Zn (Sullivan et al., 2020b), there is also an apparent lack of diurnal or postprandial variations in blood serum Cu concentrations (McMaster et al., 1992; Stengle and Schade, 1957) and isotopic compositions (Lauwens et al., 2017). Taken together, these make Cu an attractive element for isotope metallomics research.

There is a growing body of literature emerging on the application of Cu isotopic analysis in biomedicine. Forming the backbone of this research are studies that investigated factors that influence Cu isotopic compositions in the healthy state. The Cu isotope ratio has so far been demonstrated to be affected by age (Jaouen et al., 2013a; Morel et al., 2022), diet (Jaouen et al., 2017; Van Heghe et al., 2012), sex (Albarède et al., 2011; Boucher et al., 2021; Jaouen et al., 2012, 2017; Van Heghe et al., 2014), menopausal status (Jaouen and Balter, 2014; Van Heghe et al., 2014). Whereas these factors can influence the within-organ Cu isotopic composition, such changes are typically smaller than those between a given organ or fluid (Moynier et al., 2022). The δ^{65}Cu values of organs and fluids tend to cluster around points that are distinct from each other and are typically limited to ~1‰ within-reservoir variations (Balter et al., 2013; Costas-Rodríguez et al., 2019; Moynier et al., 2022). Data from three separate murine model studies demonstrates that organ δ^{65}Cu values are largely consistent even when mice are fed diets with Cu isotopic compositions that differ by almost 0.5‰ (Balter et al., 2013; Costas-Rodríguez et al., 2019; Moynier et al., 2022). For example, the mean kidney δ^{65}Cu values from the three studies are 1.51 ± 0.17‰ (2SE, n = 3), 1.65 ± 0.13‰ (2SE, n = 14) and 1.74 ± 0.12‰ (2SE, n = 14) compared to mean blood plasma/serum δ^{65}Cu values of −0.61 ± 0.08‰ (2SE, n = 8) and −0.67 ± 0.10‰ (2SE, n = 7) (Balter et al., 2013; Costas-Rodríguez et al., 2019; Moynier et al., 2022).

Towards the development of diagnostic/prognostic markers of disease, the Cu isotope ratio has been demonstrated to be affected by the altered Cu homeostasis in breast cancer (Larner et al., 2015; Télouk et al., 2015), ovarian cancer (Toubhans et al., 2020), colorectal cancer (Télouk et al., 2015), colon cancer (Lauwens, 2018), hematological malignancy (Hastuti et al., 2020b), hepatocellular carcinoma (HCC) (Balter et al., 2015; Bondanese et al., 2016; Télouk et al., 2022), liver cirrhosis (Costas-Rodríguez et al., 2015; Lauwens et al., 2018), squamous cell carcinoma (Lobo et al., 2017), cholestatic liver disease (Costas-Rodríguez et al., 2019), amyotrophic lateral sclerosis (Sauzéat et al., 2018), thyroid cancer (Kazi Tani et al., 2021), bladder cancer (Wang et al., 2022b), oxidative stress (Flórez et al., 2018), macular degeneration (Aranaz et al., 2020), glaucoma (Aranaz et al., 2021), bariatric surgery recovery (Hastuti et al., 2020a), animal cancers (Gourlan et al., 2019), liver transplant recovery (Lauwens et al., 2016), Wilson's disease (Aramendía et al., 2013; García-Poyo et al., 2021; Lamboux et al., 2020; Resano et al., 2013), and Alzheimer's disease (Larner et al., 2019; Moynier et al., 2019, 2020). Below, the Cu isotope systematics of breast cancer and Wilson's disease are discussed in further detail and future avenues of research explored.

7.1. Breast cancer

The blood serum of breast cancer patients is enriched in ^{63}Cu compared to healthy controls, which in theory requires an isotopically heavy Cu reservoir in the body to maintain mass balance in the system (Larner et al., 2015; Télouk et al., 2015). However, the opposite was observed, though from a very limited dataset (one individual), as an isotopically light δ^{65}Cu value (0.35‰ lower) in a breast cancer tumour compared to adjacent histologically normal tissue (Larner et al., 2015). From this, it was suggested that Cu binding in breast cancer cells is driven by the upregulation of metallothioneins (enriched in ^{63}Cu) (Larner et al., 2019).

Based on the low δ^{65}Cu values measured in the serum of breast cancer patients compared to healthy controls, another hypothesis for the nature of the Cu binding in breast cancer cells was formulated. The second hypothesis proposes that the oxidative chelation of Cu by cytosolic lactate (resulting from anaerobic glycolysis in cancer cells) is the main driver of Cu isotope fractionation in breast cancer cells (Télouk et al., 2015; Warburg, 1956). It was suggested that the observed shift of δ^{65}Cu values in blood serum from breast cancer patients compared to healthy controls facilitates the fingerprinting of cytosolic Cu chelation by mono- and bidentate ligands. In comparison to Cu^{2+}, compounds of Cu^{+} are typically depleted in ^{65}Cu. For lactate, the combination of Cu^{2+} oxidation state dominance and binding to a side hydroxyl (high electronegativity) leads to greater preference for ^{65}Cu compared to what would be observed for Cu in a cysteine (Cu-S) bond ($\Delta^{65}Cu_{Cu\text{-}Lactate\ -\ Cys} > 1‰$) (Fujii et al., 2014; Télouk et al., 2015). Isotopically light Cu^{+} tends to evade chelation by lactate and is excreted into the bloodstream, resulting in the lower δ^{65}Cu values observed for breast cancer patients compared to healthy controls (Télouk et al., 2015).

In support of this theory, a statistically significant enrichment of ^{65}Cu is reported in HCC tumours, oral squamous cell carcinoma tissues, colon cancer, and ovarian cancer tumours compared to non-tumoural tissue (Balter et al., 2015; Lauwens, 2018; Lobo et al., 2017; Toubhans et al., 2020). Further, blood fractions from patients with HCC, oral squamous cell carcinoma, hematological malignancies, ovarian cancer, breast cancer, colorectal cancer, colon cancer, bladder cancer, and thyroid cancer have isotopically light Cu signatures relative to healthy controls, potentially indicating a common dominant Cu isotope fractionation mechanism in cancers (Fig. 5) (Balter et al., 2015; Hastuti et al., 2020b; Kazi Tani et al., 2021; Lauwens, 2018; Télouk et al., 2015; Toubhans et al., 2020; Wang et al., 2022b).

As there are very few actual measurements of δ^{65}Cu values in malignant breast tumour samples and adjacent histologically normal tissue, additional samples should be analyzed to help settle the question of what process dominates Cu binding in breast cancer cells and how the distribution of Cu isotopes changes in patients. This work should be supported by investigations to determine the key Cu binding site in breast cancer cell cytoplasm. The similar Cu isotopic signatures in tumours and serum from patients with different types of cancer suggests that the δ^{65}Cu value may be a sensitive diagnostic marker of cancers that however lacks the ability to differentiate between them. However, the combination of δ^{65}Cu with other clinical parameters shows promise in improving the diagnostic potential of the Cu isotope ratio (Hastuti et al., 2020b; Wang et al., 2022b). The area under the Receiver operator characteristic (ROC) curve (AUC) is commonly used to assess the diagnostic capability of a variable, such as Cu concentrations or

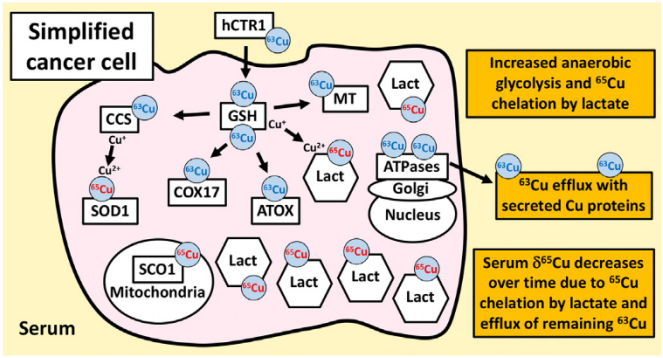

Fig. 5. Simplified model of Cu homeostasis and isotope fractionation in cancer cells. The relative enrichment of ^{65}Cu or ^{63}Cu in different molecules is shown. Copper enters the cell via human Cu transporter 1 (hCTR1), and hCTR1 or glutathione (GSH) can serve in an intermediary role to transfer Cu to copper chaperones, antioxidant 1 Cu chaperone (ATOX1), Cu chaperone for superoxide dismutase (SOD; CCS), and cytochrome C oxidase Cu chaperone (COX17), which then deliver Cu to its target proteins. Metallothionein (MT) may serve as a storage site. The target protein for CCS is SOD, COX17 targets synthesis of cytochrome C oxidase 1 (SCO1), and ATOX1 delivers Cu to the adenosinetriphosphatases (ATP7A and ATP7B). The efflux proteins, ATP7A and ATP7B, are located in the *trans*-Golgi and secretory pathway. Cytosolic Cu chelation by lactate mono- and bidentates (Lact) is proposed as the mechanism of ^{65}Cu accumulation in tumours and relative enrichment of ^{63}Cu in blood serum as isotopically light Cu^{+} tends to evade chelation by lactate and is excreted into the bloodstream. Adapted after Balter et al. (2013), Kaplan and Maryon (2016), and Wang et al. (2022b).

$\delta^{65}Cu$ values. As a recent innovation upon this, a machine learning model was developed to classify bladder cancer and non-bladder cancer subjects based on two-dimensional Cu signatures (Cu concentration and $\delta^{65}Cu$ values in blood plasma and red blood cells) (Wang et al., 2022b). The AUC of the machine learning model was distinctly greater than those generated without machine learning, with a high sensitivity, high true negative rate, and low false positive rate for the diagnosis of bladder cancer (Wang et al., 2022b). This provides a strong case for the application of machine learning in future studies investigating the diagnostic potential of the Cu isotope ratio in breast cancer or other diseases.

7.2. Wilson's disease

Wilson's disease (WD), a hereditary Cu metabolism disorder, is typified by excess Cu accumulation in the liver. Copper is incorporated into ceruloplasmin, the main Cu-binding protein in blood serum (Prohaska and Gybina, 2004), with the help of Cu-transporting adenosinetriphosphatase (ATP7B), which also facilitates its removal from the liver through secretion into bile to be stored in the gall bladder and excreted via feces (La Fontaine et al., 2010). Wilson's disease patients have a mutation in the ATP7B gene, which encodes the ATP7B protein, and (1) causes ceruloplasmin to be secreted in a form that lacks Cu and quickly breaks down in the bloodstream, and (2) disrupts the excretion of liver Cu in bile (Gitlin, 2003). Together, these result in the gradual accumulation of Cu in the liver, and lead to hepatocyte dysfunction, cell death, and the eventual release of Cu into the bloodstream and accumulation in other parts of the body (Bull et al., 1993; Gitlin, 2003; Tanzi et al., 1993). As such, patients with WD can have Cu liver concentrations as high as 5000 μg g^{-1}, compared to a range of 12.5 μg g^{-1} to 80.8 μg g^{-1} (average of 34.9 μg g^{-1}) in subjects who had no evidence of liver disease and normal liver histology (Ferenci et al., 2005).

Thus far, four studies have investigated Cu isotope fractionation induced by WD (Aramendía et al., 2013; García-Poyo et al., 2021; Lamboux et al., 2020; Resano et al., 2013). In a pilot study, the $\delta^{65}Cu$ values of blood serum from treated WD patients were enriched in lighter ^{63}Cu compared to healthy controls (Aramendía et al., 2013), and this was later suggested to be due to the low efficiency of Cu incorporation into ceruloplasmin in WD patients and the impairment of Cu excretion in bile, which is relatively enriched in ^{63}Cu (Costas-Rodríguez et al., 2019). Blocked biliary flow by bile duct ligation has been demonstrated to result in the accumulation of ^{63}Cu in the liver and the general accumulation of ^{63}Cu in the body, and may help explain the light Cu isotopic composition observed in the serum of WD patients (Costas-Rodríguez et al., 2019). However, just as the hyperaccumulation of Cu in the liver of WD patients is accompanied by the depletion of Cu in blood serum (Aramendía et al., 2013; Ferenci et al., 2005), the relative enrichment of ^{63}Cu in blood serum must be accompanied by a relative enrichment of ^{65}Cu elsewhere in the body to preserve the mass balance of the system.

Conversely, the Cu isotopic composition of whole blood from untreated or treated WD patients and healthy controls was shown to be indistinguishable, although the $\delta^{65}Cu$ value of whole blood decreased with the degree of liver fibrosis and the gradient of the phenotypic presentation, suggesting that WD progression can be monitored using the whole blood $\delta^{65}Cu$ determination (Lamboux et al., 2020). The discrepancy between the results of Aramendía et al. (2013) and Lamboux et al. (2020) may potentially be accounted for by the differences between sample types, with whole blood being a significantly larger reservoir of Cu than blood serum which would require a much larger effect to shift its $\delta^{65}Cu$.

Currently, a common test for diagnosing WD is the determination of the amount of Cu excreted in urine over 24 h. Innovating upon this, there have been efforts towards investigating the direct determination of Cu isotope ratios in dried urine spots by LA-MC-ICP-MS as a diagnostic marker of WD (Resano et al., 2013). Using 300 μl of urine, a significant decrease in $\delta^{65}Cu$ was observed in untreated WD patients compared to treated patients and healthy controls, in agreement with the findings of Aramendía et al. (2013). Another advance towards diagnosing WD using low sample volumes was made by García-Poyo et al. (2021), who innovated the determination of Cu concentrations by direct microinjection of 1 μl of serum into an ICP-MS and the use of femtosecond LA-MC-ICP-MS for the Cu isotopic analysis of dried 2 to 15 μl droplets. In this study, WD patients were either untreated (sampled at the moment of diagnosis), treated with chelators to increase Cu excretion from the liver, or treated with Zn salts to block Cu absorption. All groups except WD patients undergoing a chelating treatment had serum $\delta^{65}Cu$ values of around 0‰ or positive, indicating the preferential accumulation of ^{63}Cu in the liver, whereas those treated with chelators mostly had negative $\delta^{65}Cu$ values. These results are inconsistent with the blood serum and urine findings of Aramendía et al. (2013) and Resano et al. (2013), which indicate that ^{65}Cu must be preferentially accumulated in the liver of WD patients to preserve the mass balance of the system; however, this discrepancy was not discussed. The results of García-Poyo et al. (2021) indicate that ^{63}Cu is preferentially released by the liver with the use of a chelating agent or in the case of advanced liver damage, and show the potential to follow up on the evolution of treatment.

Conflicting Cu isotope data from WD patients so far complicates the use of $\delta^{65}Cu$ as a diagnostic/prognostic marker. Wilson's disease can be diagnosed with the help of Cu concentrations in liver biopsies, but Cu concentrations in the liver are insufficient to make a WD diagnosis alone (Ferenci et al., 2005). Characterizing the Cu isotopic composition of the WD liver could elucidate the distribution of Cu isotopes in this condition that so far remains obscured, and indicate the potential of $\delta^{65}Cu$ to serve as a diagnostic marker of WD (Sullivan et al., 2020a). Further, an approach to WD diagnosis consisting of Cu mass fraction and isotopic analysis of liver biopsies could further justify the invasive surgical procedure and provide greater sensitivity and specificity. Finally, larger-scale studies involving Cu isotope ratio determination in the liver biopsies, blood serum, and urine of treated and untreated WD patients and healthy controls are required to resolve conflicts that remain between studies and advance this potential diagnostic/prognostic tool past the pilot stage.

8. Conclusions

Interest in Cu isotopic analysis has increased significantly over the last 20 years, translating into a large body of research. Recently, it has been applied in novel ways as a (1) mineral exploration tool for vectoring towards

concealed ore deposits, (2) tracer of Cu contamination in the environment, and (3) diagnostic/prognostic marker of multiple cancers and other diseases. However, studies still generally report δ^{65}Cu values from a relatively small number of samples, which limits conclusions that can be drawn. The biggest barrier to improving sample throughput is the time required for sample preparation and analysis, but this can be reduced though the optimization of chromatography methods and automation. Improvements can yet be made to other aspects of Cu isotopic analysis, and researchers must take measures to ensure contamination and isotope fractionation during sampling and purification are minimized. This is an especially important consideration in the case of blood collection tubes, which contain additives and are not specifically designed for trace element or isotopic analysis. Contamination of biologically-relevant elements should be quantified in BCTs to allow an informed selection of the optimal BCT for specific experiments, and this will support the methodological standardization of isotope metallomics studies. Further interlaboratory comparisons of reference materials will also be important for ensuring that reproducible results can be achieved for Cu isotope ratio measurements in new material types as the application of the Cu isotope ratio expands. Finally, a lack of studies on Cu isotope fractionation during adsorption onto mineral surfaces limits our understanding of the transport of Cu in the Earth surface environment. Investigations of Cu isotope fractionation during adsorption onto minerals that play an important role in metal adsorption in soils should be prioritized. Taken together, these measures will improve our ability to interpret results and perform routine, high accuracy and precision measurements of the Cu isotope ratio in low-Cu samples, thus opening the doors to new, exciting applications.

Credit authorship contribution statement

K. Sullivan: Conceptualization, Data curation, Formal analysis, Investigation, Methodology, Project administration, Software, Visualization, Writing – original draft, Writing – review & editing. J.A. Kidder: Conceptualization, Data curation, Formal analysis, Investigation, Methodology, Project administration, Software, Visualization, Writing – original draft, Writing – review & editing. T. Junqueira: Investigation, Writing – original draft, Writing – review & editing. F. Vanhaecke: Writing – review & editing. M.I. Leybourne: Conceptualization, Project administration, Writing – original draft, Writing – review & editing.

Declaration of competing interest

The authors declare that they have no known competing financial interests or personal relationships that could have appeared to influence the work reported in this paper.

Acknowledgements

KS acknowledges funding from the Mitacs Elevate Fellowship and IGO Ltd., as well as the Special Research Fund (BOF) of Ghent University. The authors would like to thank Ryan Mathur and two anonymous reviewers for their time and efforts spent helping to improve the quality of this manuscript. This is Natural Resources Canada contribution 20210714. The authors would like to thank Jan Peter of the Geological Survey of Canada for reviewing this manuscript and providing helpful comments.

Appendix A. Supplementary data

Supplementary data to this article can be found online at https://doi.org/10.1016/j.scitotenv.2022.156084.

References

Albarède, F., 2015. Metal stable isotopes in the human body: a tribute of geochemistry to medicine. Elements 11, 265–269. https://doi.org/10.2113/gselements.11.4.265.

Albarède, F., Telouk, P., Lamboux, A., Jaouen, K., Balter, V., 2011. Isotopic evidence of unaccounted for Fe and Cu erythropoietic pathways. Metallomics 3, 926–933. https://doi.org/10.1039/C1MT00025J.

Albarède, F., Télouk, P., Balter, V., 2017. Medical applications of isotope metallomics. Rev. Mineral. Geochem. 82, 851–885. https://doi.org/10.2138/rmg.2017.82.20.

Aramendía, M., Rello, L., Resano, M., Vanhaecke, F., 2013. Isotopic analysis of Cu in serum samples for diagnosis of Wilson's disease: a pilot study. J. Anal. At. Spectrom. 28, 675–681. https://doi.org/10.1039/C3JA30349G.

Aranaz, M., Costas-Rodríguez, M., Lobo, L., González-Iglesias, H., Vanhaecke, F., Pereiro, R., 2020. Pilot study of homeostatic alterations of mineral elements in serum of patients with age-related macular degeneration via elemental and isotopic analysis using ICP-mass spectrometry. J. Pharm. Biomed. Anal. 177, 112857. https://doi.org/10.1016/j.jpba.2019.112857.

Aranaz, M., Costas-Rodríguez, M., Lobo, L., García, M., González-Iglesias, H., Pereiro, R., Vanhaecke, F., 2021. Homeostatic alterations related to total antioxidant capacity, elemental concentrations and isotopic compositions in aqueous humor of glaucoma patients. Anal. Bioanal. Chem. https://doi.org/10.1007/s00216-021-03467-5.

Araújo, D.F., Ponzevera, E., Briant, N., Knoery, J., Bruzac, S., Sireau, T., Brach-Papa, C., 2019a. Copper, zinc and lead isotope signatures of sediments from a mediterranean coastal bay impacted by naval activities and urban sources. Appl. Geochem. 111, 104440. https://doi.org/10.1016/j.apgeochem.2019.104440.

Araújo, D.F., Ponzevera, E., Briant, N., Knoery, J., Sireau, T., Mojtahid, M., Metzger, E., Brach-Papa, C., 2019b. Assessment of the metal contamination evolution in the Loire estuary using Cu and Zn stable isotopes and geochemical data in sediments. Mar. Pollut. Bull. 143, 12–23. https://doi.org/10.1016/j.marpolbul.2019.04.034.

Araújo, D.F., Knoery, J., Briant, N., Ponzevera, E., Chouvelon, T., Auby, I., Yepez, S., Bruzac, S., Sireau, T., Pellouin-Grouhel, A., Akcha, F., 2021a. Metal stable isotopes in transplanted oysters as a new tool for monitoring anthropogenic metal bioaccumulation in marine environments: the case for copper. Environ. Pollut. 290, 118012. https://doi.org/10.1016/j.envpol.2021.118012.

Araújo, D.F., Ponzevera, E., Briant, N., Knoery, J., Bruzac, S., Sireau, T., Pellouin-Grouhel, A., Brach-Papa, C., 2021b. Differences in copper isotope fractionation between mussels (Regulators) and oysters (Hyperaccumulators): insights from a ten-year biomonitoring study. Environ. Sci. Technol. 55, 324–330. https://doi.org/10.1021/acs.est.0c04691.

Araújo, D.F., Knoery, J., Briant, N., Vigier, N., Ponzevera, E., 2022. "Non-traditional" stable isotopes applied to the study of trace metal contaminants in anthropized marine environments. Mar. Pollut. Bull. 175, 113398. https://doi.org/10.1016/j.marpolbul.2022.113398.

Archer, C., Vance, D., 2004. Mass discrimination correction in multiple-collector plasma source mass spectrometry: an example using Cu and Zn isotopes. J. Anal. At. Spectrom. 19, 656–665. https://doi.org/10.1039/B315853E.

Asael, D., Matthews, A., Bar-Matthews, M., Halicz, L., 2007. Copper isotope fractionation in sedimentary copper mineralization (Timna Valley, Israel). Chem. Geol. 243, 238–254. https://doi.org/10.1016/j.chemgeo.2007.06.007.

Babcsányi, I., Chabaux, F., Granet, M., Meite, F., Payraudeau, S., Duplay, J., Imfeld, G., 2016. Copper in soil fractions and runoff in a vineyard catchment: insights from copper stable isotopes. Sci. Total Environ. 557–558, 154–162. https://doi.org/10.1016/j.scitotenv.2016.03.037.

Baconnais, I., Rouxel, O., Dulaquais, G., Boye, M., 2019. Determination of the copper isotope composition of seawater revisited: a case study from the Mediterranean Sea. Chem. Geol. 511, 465–480. https://doi.org/10.1016/j.chemgeo.2018.09.009.

Baize, D., 1997. Detection of moderate contamination by trace metals in agricultural soils; detection de contaminations moderees en elements traces dans les sols agricoles. Analusis 25.

Balistrieri, L.S., Borrok, D.M., Wanty, R.B., Ridley, W.I., 2008. Fractionation of Cu and Zn isotopes during adsorption onto amorphous Fe(III) oxyhydroxide: experimental mixing of acid rock drainage and ambient river water. Geochim. Cosmochim. Acta 72, 311–328. https://doi.org/10.1016/j.gca.2007.11.013.

Balliana, E., Aramendía, M., Resano, M., Barbante, C., Vanhaecke, F., 2013. Copper and tin isotopic analysis of ancient bronzes for archaeological investigation: development and validation of a suitable analytical methodology. Anal. Bioanal. Chem. 405, 2973–2986. https://doi.org/10.1007/s00216-012-6542-1.

Balter, V., Lamboux, A., Zazzo, A., Télouk, P., Leverrier, Y., Marvel, J., P. Moloney, A., J. Monahan, F., Schmidt, O., Albarède, F., 2013. Contrasting Cu, Fe, and Zn isotopic patterns in organs and body fluids of mice and sheep, with emphasis on cellular fractionation. Metallomics 5, 1470–1482. https://doi.org/10.1039/C3MT00151B.

Balter, V., da Costa, A.N., Bondanese, V.P., Jaouen, K., Lamboux, A., Sangrajrang, S., Vincent, N., Fourel, F., Télouk, P., Gigou, M., 2015. Natural variations of copper and sulfur stable isotopes in blood of hepatocellular carcinoma patients. Proc. Natl. Acad. Sci. U. S. A. 112, 982–985.

Baxter, D.C., Rodushkin, I., Engström, E., Malinovsky, D., 2006. Revised exponential model for mass bias correction using an internal standard for isotope abundance ratio measurements by multi-collector inductively coupled plasma mass spectrometry. J. Anal. At. Spectrom. 21, 427–430. https://doi.org/10.1039/B517457K.

Bermin, J., Vance, D., Archer, C., Statham, P.J., 2006. The determination of the isotopic composition of Cu and Zn in seawater. Chemical Geology, Special Issue in Honour of R.K. O'Nions. 226, pp. 280–297. https://doi.org/10.1016/j.chemgeo.2005.09.025.

Bigalke, M., Weyer, S., Kobza, J., Wilcke, W., 2010a. Stable Cu and Zn isotope ratios as tracers of sources and transport of Cu and Zn in contaminated soil. Geochim. Cosmochim. Acta 74, 6801–6813. https://doi.org/10.1016/j.gca.2010.08.044.

Bigalke, M., Weyer, S., Wilcke, W., 2010b. Stable copper isotopes: a novel tool to trace copper behavior in hydromorphic soils. Soil Sci. Soc. Am. J. 74, 60–73. https://doi.org/10.2136/sssaj2008.0377.

Bigalke, M., Weyer, S., Wilcke, W., 2010c. Copper isotope fractionation during complexation with insolubilized humic acid. Environ. Sci. Technol. 44, 5496–5502. https://doi.org/10.1021/es1017653.

Bigalke, M., Weyer, S., Wilcke, W., 2011. Stable Cu isotope fractionation in soils during oxic weathering and podzolization. Geochim. Cosmochim. Acta 75, 3119–3134. https://doi.org/10.1016/j.gca.2011.03.005.

Bigeleisen, J., Mayer, M.G., 1947. Calculation of equilibrium constants for isotopic exchange reactions. J. Chem. Phys. 15, 261–267. https://doi.org/10.1063/1.1746492.

Bishop, M.C., Moynier, F., Weinstein, C., Fraboulet, J.-G., Wang, K., Foriel, J., 2012. The Cu isotopic composition of iron meteorites. Meteorit. Planet. Sci. 47, 268–276.

Blotevogel, S., Oliva, P., Sobanska, S., Viers, J., Vezin, H., Audry, S., Prunier, J., Darrozes, J., Orgogozo, L., Courjault-Radé, P., Schreck, E., 2018. The fate of Cu pesticides in vineyard soils: a case study using δ65Cu isotope ratios and EPR analysis. Chem. Geol. 477, 35–46. https://doi.org/10.1016/j.chemgeo.2017.11.032.

Blotevogel, S., Schreck, E., Audry, S., Saldi, G.D., Viers, J., Courjault-Radé, P., Darrozes, J., Orgogozo, L., Oliva, P., 2019. Contribution of soil elemental contents and Cu and Sr isotope ratios to the understanding of pedogenetic processes and mechanisms involved in the soil-to-grape transfer (Soave vineyard, Italy). Geoderma 343, 72–85. https://doi.org/10.1016/j.geoderma.2019.02.015.

Blotevogel, S., Oliva, P., Denaix, L., Audry, S., Viers, J., Schreck, E., 2022. Stable Cu isotope ratios show changes in Cu uptake and transport mechanisms in Vitis vinifera due to high Cu exposure. Front. Plant Sci. 3108.

Bondanese, V.P., Lamboux, A., Simon, M., E. Lafont, J., Albalat, E., Pichat, S., Vanacker, J.-M., Telouk, P., Balter, V., Oger, P., Albarède, F., 2016. Hypoxia induces copper stable isotope fractionation in hepatocellular carcinoma, in a HIF-independent manner. Metallomics 8, 1177–1184. https://doi.org/10.1039/C6MT00102E.

Borrok, D.M., Nimick, D.A., Wanty, R.B., Ridley, W.I., 2008. Isotopic variations of dissolved copper and zinc in stream waters affected by historical mining. Geochim. Cosmochim. Acta 72, 329–344. https://doi.org/10.1016/j.gca.2007.11.014.

Boucher, R.D., Alavi, S.E., de Jong, H.N., Godfrey, L.V., Vogel, E.R., 2021. Stable isotope evidence (Fe, Cu) suggests that sex, but not aging is recorded in rhesus macaque (Macaca mulatta) bone. Am. J. Phys. Anthropol. 176, 80–92. https://doi.org/10.1002/ajpa.24301.

Boyle, D.R., 2003. Preglacial Weathering of Massive Sulfide Deposits in the Bathurst Mining Camp: Economic Geology, Geochemistry, and Exploration Applications.

Braxton, D., Mathur, R., 2011. Exploration applications of copper isotopes in the supergene environment: a case study of the Bayugo porphyry copper-gold deposit, southern Philippines. Econ. Geol. 106, 1447–1463.

Brewer, G., 2003. Copper in medicine. Curr. Opin. Chem. Biol. 7, 207–212. https://doi.org/10.1016/S1367-5931(03)00018-8.

Briant, N., 2014. Devenir et biodisponibilité du Cu, Zn et TBT dans un environnement portuaire fortement contaminé: la marina de Port Camargue. 263.

Bull, P.C., Thomas, G.R., Rommens, J.M., Forbes, J.R., Cox, D.W., 1993. The Wilson disease gene is a putative copper transporting P–type ATPase similar to the Menkes gene. Nat. Genet. 5, 327.

Chen, J., Gaillrdet, J., Louvat, P., 2008. Multi-isotopic (Zn, Cu) approach for anthropogenic contamination of suspended sediments of the Seine River,France. Geochim. Cosmochim. Acta 72, A155.

Cooke, D.R., Hollings, P., Wilkinson, J.J., Tosdal, R.M., 2014. Geochemistry of porphyry deposits. Treatise on Geochemistry, Second edition Elsevier, Ltd., Oxford.

Costas-Rodríguez, M., Anoshkina, Y., Lauwens, S., Vlierberghe, H.V., Delanghe, J., Vanhaecke, F., 2015. Isotopic analysis of Cu in blood serum by multi-collector ICP-mass spectrometry: a new approach for the diagnosis and prognosis of liver cirrhosis? Metallomics 7, 491–498. https://doi.org/10.1039/C4MT00319E.

Costas-Rodríguez, M., Van Campenhout, S., Hastuti, A.A.M.B., Devisscher, L., Van Vlierberghe, H., Vanhaecke, F., 2019. Body distribution of stable copper isotopes during the progression of cholestatic liver disease induced by common bile duct ligation in mice. Metallomics 11, 1093–1103. https://doi.org/10.1039/C8MT00362A.

Deng, X.-H., Mathur, R., Li, Y., Mao, Q.-G., Wu, Y.-S., Yang, L.-Y., Chen, X., Xu, J., 2019. Copper and zinc isotope variation of the VMS mineralization in the Kalatag district, eastern Tianshan, NW China. J. Geochem. Explor. 196, 8–19.

Dong, S., Ochoa Gonzalez, R., Harrison, R.M., Green, D., North, R., Fowler, G., Weiss, D., 2017. Isotopic signatures suggest important contributions from recycled gasoline, road dust and non-exhaust traffic sources for copper, zinc and lead in PM 10 in London, United Kingdom. Atmos. Environ. 165, 88–98. https://doi.org/10.1016/j.atmosenv.2017.06.020.

Dótor-Almazán, A., Armienta-Hernández, M.A., Talavera-Mendoza, O., Ruiz, J., 2017. Geochemical behavior of Cu and sulfur isotopes in the tropical mining region of Taxco, Guerrero (southern Mexico). Chem. Geol. 471, 1–12. https://doi.org/10.1016/j.chemgeo.2017.09.005.

Du, Q., Sun, Z., Forsling, W., Tang, H., 1997. Adsorption of copper at aqueous illite surfaces. J. Colloid Interface Sci. 187, 232–242.

Duangthong, S., Rattanadaecha, K., Cheewasedtham, W., Wararattananurak, P., Chooto, P., 2017. Simple digestion and visible spectrophotometry for copper determination in natural rubber latex. ScienceAsia 43, 369–376.

Ehrlich, S., Butler, I., Halicz, L., Rickard, D., Oldroyd, A., Matthews, A., 2004. Experimental study of the copper isotope fractionation between aqueous Cu(II) and covellite, CuS. Chem. Geol. 209, 259–269. https://doi.org/10.1016/j.chemgeo.2004.06.010.

El Azzi, D., Viers, J., Guiresse, M., Probst, A., Aubert, D., Caparros, J., Charles, F., Guizien, K., Probst, J.L., 2013. Origin and fate of copper in a small Mediterranean vineyard catchment: new insights from combined chemical extraction and δ65Cu isotopic composition. Sci. Total Environ. 463–464, 91–101. https://doi.org/10.1016/j.scitotenv.2013.05.058.

Enge, T.G., Paul Field, M., F. Jolley, D., Ecroyd, H., Hwan Kim, M., Dosseto, A., 2016. An automated chromatography procedure optimized for analysis of stable Cu isotopes from biological materials. J. Anal. At. Spectrom. 31, 2023–2030. https://doi.org/10.1039/C6JA00120C.

Fekiacova, Z., Cornu, S., Pichat, S., 2015. Tracing contamination sources in soils with Cu and Zn isotopic ratios. Sci. Total Environ. 517, 96–105. https://doi.org/10.1016/j.scitotenv.2015.02.046.

Ferenci, P., Steindl-Munda, P., Vogel, W., Jessner, W., Gschwantler, M., Stauber, R., Datz, C., Hackl, F., Wrba, F., Bauer, P., 2005. Diagnostic value of quantitative hepatic copper determination in patients with Wilson's disease. Clin. Gastroenterol. Hepatol. 3, 811–818. https://doi.org/10.1016/S1542-3565(05)00181-3.

Fernandez, A., Borrok, D.M., 2009. Fractionation of Cu, Fe, and Zn isotopes during the oxidative weathering of sulfide-rich rocks. Chem. Geol. 264, 1–12. https://doi.org/10.1016/j.chemgeo.2009.01.024.

Ficklin, W.H., Plumlee, G.S., Smith, K.S., McHugh, J.B., 1992. Geochemical classification of mine drainages and natural drainages in mineralized areas. Presented at the International Symposium on Water-Rock Interaction, pp. 381–384.

Fitzgerald, D.J., 1998. Safety guidelines for copper in water. Am. J. Clin. Nutr. 67, 1098S–1102S. https://doi.org/10.1093/ajcn/67.5.1098S.

Flórez, M.R., Costas-Rodríguez, M., Grootaert, C., Van Camp, J., Vanhaecke, F., 2018. Cu isotope fractionation response to oxidative stress in a hepatic cell line studied using multi-collector ICP-mass spectrometry. Anal. Bioanal. Chem. 410, 2385–2394. https://doi.org/10.1007/s00216-018-0909-x.

Friel, J.K., Mercer, C., Andrews, W.L., Simmons, B.R., Jackson, S.E., 1996. Laboratory gloves as a source of trace element contamination. Biol. Trace Elem. Res. 54, 135–142.

Fujii, T., Moynier, F., Abe, M., Nemoto, K., Albarède, F., 2013. Copper isotope fractionation between aqueous compounds relevant to low temperature geochemistry and biology. Geochim. Cosmochim. Acta 110, 29–44. https://doi.org/10.1016/j.gca.2013.02.007.

Fujii, T., Moynier, F., Blichert-Toft, J., Albarède, F., 2014. Density functional theory estimation of isotope fractionation of Fe, Ni, Cu, and Zn among species relevant to geochemical and biological environments. Geochim. Cosmochim. Acta 140, 553–576. https://doi.org/10.1016/j.gca.2014.05.051.

Gaetke, L.M., Chow, C.K., 2003. Copper toxicity, oxidative stress, and antioxidant nutrients. Toxicol. Environ. Nutr. Interact. Antioxida. Nutr. Environ. Health, Part C 189, 147–163. https://doi.org/10.1016/S0300-483X(03)00159-8.

Gale, N.H., Woodhead, A.P., Stos-Gale, Z.A., Walder, A., Bowen, I., 1999. Natural variations detected in the isotopic composition of copper: possible applications to archaeology and geochemistry. Int. J. Mass Spectrom. 184, 1–9. https://doi.org/10.1016/S1387-3806(98)14294-X.

García-Poyo, M.C., Bérail, S., Laure Ronzani, A., Rello, L., García-González, E., Lelièvre, B., Cales, P., V. Nakadi, F., Aramendía, M., Resano, M., Pécheyran, C., 2021. Laser ablation of microdroplets for copper isotopic analysis via MC-ICP-MS. Analysis of serum microsamples for the diagnosis and follow-up treatment of Wilson's disease. J. Anal. At. Spectrom. 36, 968–980. https://doi.org/10.1039/D0JA00494D.

Gasparon, M., 1998. Trace metals in water samples: minimising contamination during sampling and storage. Environ. Geol. 36, 207–214.

Gelly, R., Fekiacova, Z., Guihou, A., Doelsch, E., Deschamps, P., Keller, C., 2019. Lead, zinc, and copper redistributions in soils along a deposition gradient from emissions of a Pb-Ag smelter decommissioned 100 years ago. Sci. Total Environ. 665, 502–512. https://doi.org/10.1016/j.scitotenv.2019.02.092.

Gitlin, J.D., 2003. Wilson disease. Gastroenterology 125, 1868–1877. https://doi.org/10.1053/j.gastro.2003.05.010.

Gonzalez, R.O., Strekopytov, S., Amato, F., Querol, X., Reche, C., Weiss, D., 2016. New insights from zinc and copper isotopic compositions into the sources of atmospheric particulate matter from two major European cities. Environ. Sci. Technol. 50, 9816–9824. https://doi.org/10.1021/acs.est.6b00863.

González-Costa, J.J., Reigosa, M.J., Matías, J.M., Fernández-Covelo, E., 2017. Analysis of the importance of oxides and clays in Cd, Cr, Cu, Ni, Pb and Zn adsorption and retention with regression trees. PLoS ONE 12, e0168523. https://doi.org/10.1371/journal.pone.0168523.

Goodfellow, W.D., 2007. Mineral Deposits of Canada: A Synthesis of Major Deposit-types, District Metallogeny, the Evolution of Geological Provinces, and Exploration Methods. Geological Association of Canada, Mineral Deposits Division.

Gourlan, A.T., Douay, G., Telouk, P., 2019. Copper isotopes as possible neoplasia biomarkers in captive wild felids. Zoo Biol. https://doi.org/10.1002/zoo.21504.

Graham, S., Pearson, N., Jackson, S., Griffin, W., O'Reilly, S.Y., 2004. Tracing Cu and Fe from source to porphyry: in situ determination of Cu and Fe isotope ratios in sulfides from the Grasberg Cu–Au deposit. Chem. Geol. 207, 147–169. https://doi.org/10.1016/j.chemgeo.2004.02.009.

Gropper, S.S., Smith, J.L., 2012. Advanced Nutrition and Human Metabolism. Cengage Learning.

Guinoiseau, D., Bouchez, J., Gélabert, A., Louvat, P., Moreira-Turcq, P., Filizola, N., Benedetti, M.F., 2018. Fate of particulate copper and zinc isotopes at the Solimões-Negro river confluence, Amazon Basin, Brazil. Chem. Geol. 489, 1–15. https://doi.org/10.1016/j.chemgeo.2018.05.004.

Haest, M., Muchez, P., Petit, J.C.J., Vanhaecke, F., 2009. Cu isotope ratio variations in the Dikulushi Cu-Ag deposit, DRC: of primary origin or induced by supergene reworking? Econ. Geol. 104, 1055–1064. https://doi.org/10.2113/econgeo.104.7.1055.

Hastuti, A.A.M.B., Costas-Rodríguez, M., Anoshkina, Y., Parnall, T., Madura, J.A., Vanhaecke, F., 2020a. High-precision isotopic analysis of serum and whole blood Cu, Fe and Zn to assess possible homeostasis alterations due to bariatric surgery. Anal. Bioanal. Chem. 412, 727–738. https://doi.org/10.1007/s00216-019-02291-2.

Hastuti, A.A.M.B., Costas-Rodríguez, M., Matsunaga, A., Ichinose, T., Hagiwara, S., Shimura, M., Vanhaecke, F., 2020b. Cu and Zn isotope ratio variations in plasma for survival prediction in hematological malignancy cases. Sci. Rep. 10, 1–12. https://doi.org/10.1038/s41598-020-71764-7.

Hou, Q., Zhou, L., Gao, S., Zhang, T., Feng, L., Yang, L., 2016. Use of Ga for mass bias correction for the accurate determination of copper isotope ratio in the NIST SRM 3114 Cu standard and geological samples by MC-ICPMS. J. Anal. At. Spectrom. 31, 280–287. https://doi.org/10.1039/C4JA00488D.

Housh, T.B., Çiftçi, E., 2008. Cu isotope geochemistry of volcanogenic massive sulphide deposits of the eastern Pontides, Turkey. IOP Conference Series: Earth and Environmental Science. IOP Publishing, p. 012025.

Ijichi, Y., Ohno, T., Sakata, S., 2018. Copper isotopic fractionation during adsorption on manganese oxide: effects of pH and desorption. Geochem. J. 52, e1–e6. https://doi.org/10.2343/geochemj.2.0516.

Ikehata, K., Notsu, K., Hirata, T., 2011. Copper isotope characteristics of copper-rich minerals from Besshi-type volcanogenic massive sulfide deposits, Japan, determined using a femtosecond LA-MC-ICP-MS. Econ. Geol. 106, 307–316.

Jaouen, K., Balter, V., 2014. Menopause effect on blood Fe and Cu isotope compositions: menopause effect on blood Fe and Cu isotopes. Am. J. Phys. Anthropol. 153, 280–285. https://doi.org/10.1002/ajpa.22430.

Jaouen, K., Balter, V., Herrscher, E., Lamboux, A., Telouk, P., Albarède, F., 2012. Fe and Cu stable isotopes in archeological human bones and their relationship to sex. Am. J. Phys. Anthropol. 148, 334–340. https://doi.org/10.1002/ajpa.22053.

Jaouen, K., Gibert, M., Lamboux, A., Telouk, P., Fourel, F., Albarède, F., N. Alekseev, A., Crubézy, E., Balter, V., 2013. Is aging recorded in blood Cu and Zn isotope compositions? Metallomics 5, 1016–1024. https://doi.org/10.1039/C3MT00085K.

Jaouen, K., Pons, M.-L., Balter, V., 2013b. Iron, copper and zinc isotopic fractionation up mammal trophic chains. Earth Planet. Sci. Lett. 374, 164–172. https://doi.org/10.1016/j.epsl.2013.05.037.

Jaouen, K., Herrscher, E., Balter, V., 2017. Copper and zinc isotope ratios in human bone and enamel. Am. J. Phys. Anthropol. 162, 491–500. https://doi.org/10.1002/ajpa.23132.

Jeong, H., Ra, K., 2021. Multi-isotope signatures (Cu, Zn, Pb) of different particle sizes in road-deposited sediments: a case study from industrial area. J. Anal. Sci. Technol. 12, 39. https://doi.org/10.1186/s40543-021-00292-4.

Jeong, H., Ra, K., Choi, J.Y., 2021. Copper, zinc and lead isotopic delta values and isotope ratios of various geological and biological reference materials. Geostand. Geoanal. Res. 45, 551–563. https://doi.org/10.1111/ggr.12379.

Jouvin, D., Weiss, D.J., Mason, T.F.M., Bravin, M.N., Louvat, P., Zhao, F., Ferec, F., Hinsinger, P., Benedetti, M.F., 2012. Stable isotopes of Cu and Zn in higher plants: evidence for Cu reduction at the root surface and two conceptual models for isotopic fractionation processes. Environ. Sci. Technol. 46, 2652–2660. https://doi.org/10.1021/es202587m.

Kaplan, J.H., Maryon, E.B., 2016. How mammalian cells acquire copper: an essential but potentially toxic metal. Biophys. J. 110 (1), 7–13. https://doi.org/10.1016/j.bpj.2015.11.025.

Kazi Tani, L.S., Gourlan, A.T., Dennouni-Medjati, N., Telouk, P., Dali-Sahi, M., Harek, Y., Sun, Q., Hackler, J., Belhadj, M., Schomburg, L., Charlet, L., 2021. Copper isotopes and copper to zinc ratio as possible biomarkers for thyroid cancer. Front. Med. 8, 698167. https://doi.org/10.3389/fmed.2021.698167.

Kidder, J.A., Voinot, A., Sullivan, K.V., Chipley, D., Valentino, M., Layton-Matthews, D., Leybourne, M., 2020. Improved ion-exchange column chromatography for Cu purification from high-Na matrices and isotopic analysis by MC-ICPMS. J. Anal. At. Spectrom. 35, 776–783. https://doi.org/10.1039/C9JA00359B.

Kidder, J.A., Voinot, A., Leybourne, M.I., Layton-Matthews, D., Bowell, R.J., 2021. Using stable isotopes of Cu, Mo, S, and 87Sr/86Sr in hydrogeochemical mineral exploration as tracers of porphyry and exotic copper deposits. Appl. Geochem. 104935. https://doi.org/10.1016/j.apgeochem.2021.104935.

Kidder, J.A., Sullivan, K., Leybourne, M.I., Voinot, A., Layton-Matthews, D., Stoltze, A., Bowell, R.J., 2022. Hydrogeochemical mineral exploration in deeply weathered terrains: an example from Mumbwa,Zambia. Sci. Total Environ. 810, 151215. https://doi.org/10.1016/j.scitotenv.2021.151215.

Kim, B.-E., Nevitt, T., Thiele, D.J., 2008. Mechanisms for copper acquisition, distribution and regulation. Nat. Chem. Biol. 4, 176–185. https://doi.org/10.1038/nchembio.72.

Kimball, B.E., Mathur, R., Dohnalkova, A.C., Wall, A.J., Runkel, R.L., Brantley, S.L., 2009. Copper isotope fractionation in acid mine drainage. Geochim. Cosmochim. Acta 73, 1247–1263. https://doi.org/10.1016/j.gca.2008.11.035.

Komárek, M., Ratié, G., Vaňková, Z., Šípková, A., Chrastný, V., 2021. Metal isotope complexation with environmentally relevant surfaces: opening the isotope fractionation black box. Crit. Rev. Environ. Sci. Technol., 1–31 https://doi.org/10.1080/10643389.2021.1955601.

Kříbek, B., Šípková, A., Ettler, V., Mihaljevič, M., Majer, V., Knésl, I., Mapani, B., Penížek, V., Vaněk, A., Sracek, O., 2018. Variability of the copper isotopic composition in soil and grass affected by mining and smelting in Tsumeb, Namibia. Chem. Geol. 493, 121–135. https://doi.org/10.1016/j.chemgeo.2018.05.035.

Kusonwiriyawong, C., Bigalke, M., Abgottspon, F., Lazarov, M., Schuth, S., Weyer, S., Wilcke, W., 2017. Isotopic variation of dissolved and colloidal iron and copper in a carbonatic floodplain soil after experimental flooding. Chem. Geol. 459, 13–23.

Kyser, K., Lahusen, L., Drever, G., Dunn, C., Leduc, E., Chipley, D., 2015. Using Pb isotopes in surface media to distinguish anthropogenic sources from undercover uranium sources. Compt. Rendus Geosci. 347, 215–226. https://doi.org/10.1016/j.crte.2015.06.003.

La Fontaine, S., Ackland, M.L., Mercer, J.F., 2010. Mammalian copper-transporting P-type ATPases, ATP7A and ATP7B: emerging roles. Int. J. Biochem. Cell Biol. 42, 206–209.

Lamboux, A., Couchonnal-Bedoya, E., Guillaud, O., Laurencin, C., Lion-Francois, L., Belmalih, A., Mintz, E., Brun, V., Bost, M., Lachaux, A., Balter, V., 2020. The blood copper isotopic composition is a prognostic indicator of the hepatic injury in Wilson disease. Metallomics 12, 1781–1790. https://doi.org/10.1039/D0MT00167H.

Larner, F., N. Woodley, L., Shousha, S., Moyes, A., Humphreys-Williams, E., Strekopytov, S., N. Halliday, A., Rehkämper, M., Charles Coombes, R., 2015. Zinc isotopic compositions of breast cancer tissue. Metallomics 7, 112–117. https://doi.org/10.1039/C4MT00260A.

Larner, F., McLean, C.A., Halliday, A.N., Roberts, B.R., 2019. Copper isotope compositions of superoxide dismutase and metallothionein from post-mortem human frontal cortex. Inorganics 7, 86. https://doi.org/10.3390/inorganics7070086.

Larson, P.B., Maher, K., Ramos, F.C., Chang, Z., Gaspar, M., Meinert, L.D., 2003. Copper isotope ratios in magmatic and hydrothermal ore-forming environments. Chem. Geol. 201, 337–350. https://doi.org/10.1016/j.chemgeo.2003.08.006.

Lauwens, S., 2018. The Development and Evaluation of Analytical Methods for High-precision Isotopic Analysis of Cu via Multi-collector Inductively Coupled Plasma-mass Spectrometry for Biomedical Investigations. (PhD Thesis)Ghent University.

Lauwens, S., Costas-Rodríguez, M., Vlierberghe, H.V., Vanhaecke, F., 2016. Cu isotopic signature in blood serum of liver transplant patients: a follow-up study. Sci. Rep. 6, 1–9. https://doi.org/10.1038/srep30683.

Lauwens, S., Costas-Rodríguez, M., Van Vlierberghe, H., Vanhaecke, F., 2017. High-precision isotopic analysis of Cu in blood serum via multi-collector ICP-mass spectrometry for clinical investigation: steps towards improved robustness and higher sample throughput. J. Anal. At. Spectrom. 32, 597–608. https://doi.org/10.1039/C6JA00433D.

Lauwens, S., Costas-Rodríguez, M., Delanghe, J., Van Vlierberghe, H., Vanhaecke, F., 2018. Quantification and isotopic analysis of bulk and of exchangeable and ultrafiltrable serum copper in healthy and alcoholic cirrhosis subjects. Talanta 189, 332–338. https://doi.org/10.1016/j.talanta.2018.07.011.

Li, W., Jackson, S.E., Pearson, N.J., Graham, S., 2010. Copper isotopic zonation in the Northparkes porphyry Cu–Au deposit, SE Australia. Geochim. Cosmochim. Acta 74, 4078–4096.

Li, D., Liu, S.-A., Li, S., 2015. Copper isotope fractionation during adsorption onto kaolinite: experimental approach and applications. Chem. Geol. 396, 74–82. https://doi.org/10.1016/j.chemgeo.2014.12.020.

Li, S.-Z., Zhu, X.-K., Wu, L.-H., Luo, Y.-M., 2016. Cu isotopic compositions in Elsholtzia splendens: influence of soil condition and growth period on Cu isotopic fractionation in plant tissue. Chem. Geol. 444, 49–58. https://doi.org/10.1016/j.chemgeo.2016.09.036.

Li, S.-Z., Zhu, X.-K., Wu, L.-H., Luo, Y.-M., 2020. Zinc, iron, and copper isotopic fractionation in Elsholtzia splendens Nakai: a study of elemental uptake and (re)translocation mechanisms. J. Asian Earth Sci. 192, 104227. https://doi.org/10.1016/j.jseaes.2020.104227.

Lichtner, P.C., Biino, G.G., 1992. A first principles approach to supergene enrichment of a porphyry copper protore: I.Cu-Fe-S subsystem. Geochim. Cosmochim. Acta 56, 3987–4013.

Little, S.H., Sherman, D.M., Vance, D., Hein, J.R., 2014a. Molecular controls on Cu and Zn isotopic fractionation in Fe–Mn crusts. Earth Planet. Sci. Lett. 396, 213–222. https://doi.org/10.1016/j.epsl.2014.04.021.

Little, S.H., Vance, D., Walker-Brown, C., Landing, W.M., 2014. The oceanic mass balance of copper and zinc isotopes, investigated by analysis of their inputs, and outputs to ferromanganese oxide sediments. Geochim. Cosmochim. Acta 21.

Little, S.H., Archer, C., Milne, A., Schlosser, C., Achterberg, E.P., Lohan, M.C., Vance, D., 2018. Paired dissolved and particulate phase Cu isotope distributions in the South Atlantic. Chem. Geol. 502, 29–43. https://doi.org/10.1016/j.chemgeo.2018.07.022.

Liu, S.-A., Li, D., Li, S., Teng, F., Ke, S., He, Y., Lu, Y., 2014. High-precision copper and iron isotope analysis of igneous rock standards by MC-ICP-MS. J. Anal. At. Spectrom. 29, 122–133. https://doi.org/10.1039/C3JA50232E.

Liu, S.-A., Huang, J., Liu, J., Wörner, G., Yang, W., Tang, Y.-J., Chen, Y., Tang, L., Zheng, J., Li, S., 2015. Copper isotopic composition of the silicate Earth. Earth Planet. Sci. Lett. 427, 95–103. https://doi.org/10.1016/j.epsl.2015.06.061.

Liu, S., Li, Y., Liu, Jie, Yang, Z., Liu, Jianming, Shi, Y., 2021. Equilibrium Cu isotope fractionation in copper minerals: a first-principles study. Chem. Geol. 564, 120060. https://doi.org/10.1016/j.chemgeo.2021.120060.

Lobo, L., Costas-Rodríguez, M., de Vicente, J.C., Pereiro, R., Vanhaecke, F., Sanz-Medel, A., 2017. Elemental and isotopic analysis of oral squamous cell carcinoma tissues using sector-field and multi-collector ICP-mass spectrometry. Talanta 165, 92–97. https://doi.org/10.1016/j.talanta.2016.12.007.

Mahan, B., Chung, R.S., Pountney, D.L., Moynier, F., Turner, S., 2020. Isotope metallomics approaches for medical research. Cell. Mol. Life Sci. 77, 3293–3309. https://doi.org/10.1007/s00018-020-03484-0.

Malitch, K.N., Latypov, R.M., Badanina, I.Y., Sluzhenikin, S.F., 2014. Insights into ore genesis of Ni-Cu-PGE sulfide deposits of the Noril'sk province (Russia): evidence from copper and sulfur isotopes. Lithos 204, 172–187.

Maréchal, C., Albarède, F., 2002. Ion-exchange fractionation of copper and zinc isotopes. Geochim. Cosmochim. Acta 66, 1499–1509. https://doi.org/10.1016/S0016-7037(01)00815-8.

Maréchal, C.N., Télouk, P., Albarède, F., 1999. Precise analysis of copper and zinc isotopic compositions by plasma-source mass spectrometry. Chem. Geol. 156, 251–273. https://doi.org/10.1016/S0009-2541(98)00191-0.

Masbou, J., Viers, J., Grande, J.-A., Freydier, R., Zouiten, C., Seyler, P., Pokrovsky, O.S., Behra, P., Dubreuil, B., de la Torre, M.-L., 2020. Strong temporal and spatial variation of dissolved Cu isotope composition in acid mine drainage under contrasted hydrological conditions. Environ. Pollut. 266, 115104. https://doi.org/10.1016/j.envpol.2020.115104.

Mason, T.F., Weiss, D.J., Chapman, J.B., Wilkinson, J.J., Tessalina, S.G., Spiro, B., Horstwood, M.S., Spratt, J., Coles, B.J., 2005. Zn and Cu isotopic variability in the Alexandrinka volcanic-hosted massive sulphide (VHMS) ore deposit, Urals, Russia. Chem. Geol. 221, 170–187.

Mathur, R., Ruiz, J., Titley, S., Liermann, L., Buss, H., Brantley, S., 2005. Cu isotopic fractionation in the supergene environment with and without bacteria. Geochim. Cosmochim. Acta 69, 5233–5246. https://doi.org/10.1016/j.gca.2005.06.022.

Mathur, R., Titley, S., Barra, F., Brantley, S., Wilson, M., Phillips, A., Munizaga, F., Maksaev, V., Vervoort, J., Hart, G., 2009. Exploration potential of Cu isotope fractionation in porphyry copper deposits. J. Geochem. Explor. 102, 1–6. https://doi.org/10.1016/j.gexplo.2008.09.004.

Mathur, R., Dendas, M., Titley, S., Phillips, A., 2010. Patterns in the copper isotope composition of minerals in porphyry copper deposits in southwestern United States. Econ. Geol. 105, 1457–1467. https://doi.org/10.2113/econgeo.105.8.1457.

Mathur, R., Ruiz, J., Casselman, M.J., Megaw, P., van Egmond, R., 2012. Use of Cu isotopes to distinguish primary and secondary Cu mineralization in the Cañariaco Norte porphyry copper deposit, Northern Peru. Mineral. Deposita 47, 755–762. https://doi.org/10.1007/s00126-012-0439-y.

Mathur, R., Munk, L., Nguyen, M., Gregory, M., Annell, H., Lang, J., 2013. Modern and paleofluid pathways revealed by Cu isotope compositions in surface waters and ores of the pebble porphyry Cu-Au-Mo deposit, Alaska. Econ. Geol. 108, 529–541. https://doi.org/10.2113/econgeo.108.3.529.

Mathur, R., Munk, L.A., Townley, B., Gou, K.Y., Gómez Miguélez, N., Titley, S., Chen, G.G., Song, S., Reich, M., Tornos, F., Ruiz, J., 2014. Tracing low-temperature aqueous metal migration in mineralized watersheds with Cu isotope fractionation. Appl. Geochem. 51, 109–115. https://doi.org/10.1016/j.apgeochem.2014.09.019.

Mattielli, N., Rimetz, J., Petit, J., Perdrix, E., Deboudt, K., Flament, P., Weis, D., 2006. Zn–Cu isotopic study and speciation of airborne metal particles within a 5-km zone of a lead/zinc smelter. Geochim. Cosmochim. Acta 70, A401. https://doi.org/10.1016/j.gca.2006.06.808.

McMaster, D., McCrum, E., Patterson, C.C., Kerr, M.M., O'Reilly, D., Evans, A.E., Love, A.H., 1992. Serum copper and zinc in random samples of the population of Northern Ireland. Am. J. Clin. Nutr. 56, 440–446.

Meynadier, L., Gorge, C., Birck, J.-L., Allègre, C.J., 2006. Automated separation of Sr from natural water samples or carbonate rocks by high performance ion chromatography. Chem. Geol. 227, 26–36.

Miguélez, N.G., Arroyo, F.T., Velasco, F., Videira, J.C., 2019. Geology and Cu Isotope Geochemistry of the Las Cruces Deposit (SW Spain).

Mihaljevič, M., Jarošíková, A., Ettler, V., Vaněk, A., Penížek, V., Kříbek, B., Chrastný, V., Sracek, O., Trubač, J., Svoboda, M., Nyambe, I., 2018. Copper isotopic record in soils and tree rings near a copper smelter, Copperbelt, Zambia. Sci. Total Environ. 621, 9–17. https://doi.org/10.1016/j.scitotenv.2017.11.114.

Mihaljevič, M., Baieta, R., Ettler, V., Vaněk, A., Kříbek, B., Penížek, V., Drahota, P., Trubač, J., Sracek, O., Chrastný, V., Mapani, B.S., 2019. Tracing the metal dynamics in semi-arid soils near mine tailings using stable Cu and Pb isotopes. Chem. Geol. 515, 61–76. https://doi.org/10.1016/j.chemgeo.2019.03.026.

Mirnejad, H., Mathur, R., Einali, M., Dendas, M., Alirezaei, S., 2010. A comparative copper isotope study of porphyry copper deposits in Iran. Geochem.: Explor., Environ., Anal. 10, 413–418.

Morel, J.-D., Sauzéat, L., Goeminne, L.J.E., Jha, P., Williams, E., Houtkooper, R.H., Aebersold, R., Auwerx, J., Balter, V., 2022. The mouse metallomic landscape of aging and metabolism. Nat. Commun. 13, 607. https://doi.org/10.1038/s41467-022-28060-x.

Moynier, F., Vance, D., Fujii, T., Savage, P., 2017. The isotope geochemistry of zinc and copper. Rev. Mineral. Geochem. 82, 543–600. https://doi.org/10.2138/rmg.2017.82.13.

Moynier, F., Creech, J., Dallas, J., Le Borgne, M., 2019. Serum and brain natural copper stable isotopes in a mouse model of Alzheimer's disease. Sci. Rep. 9, 1–7.

Moynier, F., Borgne, M.L., Laoud, E., Mahan, B., Mouton-Ligier, F., Hugon, J., Paquet, C., 2020. Copper and zinc isotopic excursions in the human brain affected by Alzheimer's disease. Alzheimer Dement. Diagn. Assess. Dis. Monit. 12, e12112. https://doi.org/10.1002/dad2.12112.

Moynier, F., Merland, A., Rigoussen, D., Moureau, J., Paquet, M., Mahan, B., Borgne, M.L., 2022. Baseline distribution of stable copper isotope compositions of the brain and other organs in mice. Metallomics, mfac017 https://doi.org/10.1093/mtomcs/mfac017.

Navarrete, J.U., Borrok, D.M., Viveros, M., Ellzey, J.T., 2011a. Copper isotope fractionation during surface adsorption and intracellular incorporation by bacteria. Geochim. Cosmochim. Acta 75, 784–799. https://doi.org/10.1016/j.gca.2010.11.011.

Navarrete, J.U., Viveros, M., Ellzey, J.T., Borrok, D.M., 2011b. Copper isotope fractionation by desert shrubs. Appl. Geochem. 26, S319–S321. https://doi.org/10.1016/j.apgeochem.2011.04.002.

Novak, M., Sipkova, A., Chrastny, V., Stepanova, M., Voldrichova, P., Veselovsky, F., Prechova, E., Blaha, V., Curik, J., Farkas, J., Erbanova, L., Bohdalkova, L., Pasava, J., Mikova, J., Komarek, A., Krachler, M., 2016. Cu-Zn isotope constraints on the provenance of air pollution in Central Europe: using soluble and insoluble particles in snow and rime. Environ. Pollut. 218, 1135–1146. https://doi.org/10.1016/j.envpol.2016.08.067.

Palacios, C., Rouxel, O., Reich, M., Cameron, E.M., Leybourne, M.I., 2011. Pleistocene recycling of copper at a porphyry system, Atacama Desert, Chile: Cu isotope evidence. Mineral. Deposita 46, 1–7. https://doi.org/10.1007/s00126-010-0315-6.

Pallavicini, N., Engström, E., Baxter, D.C., Öhlander, B., Ingri, J., Hawley, S., Hirst, C., Rodushkina, K., Rodushkin, I., 2018. Ranges of B, Cd, Cr, Cu, Fe, Pb, Sr, Tl, and Zn concentrations and isotope ratios in environmental matrices from an urban area. J. Spectrosc. 2018, e7408767. https://doi.org/10.1155/2018/7408767.

Pękala, M., Asael, D., Butler, I.B., Matthews, A., Rickard, D., 2011. Experimental study of Cu isotope fractionation during the reaction of aqueous Cu(II) with Fe(II) sulphides at temperatures between 40 and 200°C. Chem. Geol. 289, 31–38. https://doi.org/10.1016/j.chemgeo.2011.07.004.

Pérez Rodríguez, N., Engström, E., Rodushkin, I., Nason, P., Alakangas, L., Öhlander, B., 2013. Copper and iron isotope fractionation in mine tailings at the Laver and Kristineberg mines, northern Sweden. Appl. Geochem. 32, 204–215. https://doi.org/10.1016/j.apgeochem.2012.10.012.

Petit, J.C.J., Jong, J.D., Chou, L., Mattielli, N., 2008. Development of Cu and Zn isotope MC-ICP-MS measurements: application to suspended particulate matter and sediments from the Scheldt Estuary. Geostand. Geoanal. Res. 32, 149–166. https://doi.org/10.1111/j.1751-908X.2008.00867.x.

Petit, J.C.J., Schäfer, J., Coynel, A., Blanc, G., Deycard, V.N., Derriennic, H., Lanceleur, L., Dutruch, L., Bossy, C., Mattielli, N., 2013. Anthropogenic sources and biogeochemical reactivity of particulate and dissolved cu isotopes in the turbidity gradient of the Garonne River (France). Chem. Geol. 359, 125–135. https://doi.org/10.1016/j.chemgeo.2013.09.019.

Plumlee, G.S., Smith, K.S., Montour, M.R., Ficklin, W.H., Mosier, E.L., 1999. Chapter 19 Geologic Controls on the Composition of Natural Waters and Mine Waters Draining Diverse Mineral-Deposit Types.

Pokrovsky, O.S., Viers, J., Emnova, E.E., Kompantseva, E.I., Freydier, R., 2008. Copper isotope fractionation during its interaction with soil and aquatic microorganisms and metal oxy (hydr)oxides: possible structural control. Geochim. Cosmochim. Acta 72, 1742–1757. https://doi.org/10.1016/j.gca.2008.01.018.

Pontér, S., Sutliff-Johansson, S., Engström, E., Widerlund, A., Mäki, A., Rodushkina, K., Paulukat, C., Rodushkin, I., 2021. Evaluation of a multi-isotope approach as a complement to concentration data within environmental forensics. Minerals 11, 37. https://doi.org/10.3390/min11010037.

Prohaska, J.R., Gybina, A.A., 2004. Intracellular copper transport in mammals. J. Nutr. 134, 1003–1006.

Qi, D., Behrens, H., Lazarov, M., Weyer, S., 2019. Cu isotope fractionation during reduction processes in aqueous systems: evidences from electrochemical deposition. Contrib. Mineral. Petrol. 174, 1–18.

Rauch, J.N., Pacyna, J.M., 2009. Earth's global Ag, Al, Cr, Cu, Fe, Ni, Pb, and Zn cycles. Glob. Biogeochem. Cycles 23. https://doi.org/10.1029/2008GB003376.

Reich, M., Palacios, C., Vargas, G., Luo, S., Cameron, E.M., Leybourne, M.I., Parada, M.A., Zúñiga, A., You, C.-F., 2009. Supergene enrichment of copper deposits since the onset of modern hyperaridity in the Atacama Desert, Chile. Mineral. Deposita 44, 497–504.

Resano, M., Aramendía, M., Rello, L., Calvo, M.L., Bérail, S., Pécheyran, C., 2013. Direct determination of Cu isotope ratios in dried urine spots by means of fs-LA-MC-ICPMS. Potential to diagnose Wilson's disease. J. Anal. At. Spectrom. 28, 98–106.

Retzmann, A., Zimmermann, T., Pröfrock, D., Prohaska, T., Irrgeher, J., 2017. A fully automated simultaneous single-stage separation of Sr, Pb, and Nd using DGA resin for the isotopic analysis of marine sediments. Anal. Bioanal. Chem. 409, 5463–5480.

Richards, J.P., 2021. Porphyry copper deposit formation in arcs: what are the odds? Geosphere https://doi.org/10.1130/GES02086.1.

Roebbert, Y., Rabe, K., Lazarov, M., Schuth, S., Schippers, A., Dold, B., Weyer, S., 2018. Fractionation of Fe and Cu isotopes in acid mine tailings: modification and application of a sequential extraction method. Chem. Geol. 493, 67–79. https://doi.org/10.1016/j.chemgeo.2018.05.026.

Romaniello, S.J., Field, M.P., Smith, H.B., Gordon, G.W., Kim, M.H., Anbar, A.D., 2015. Fully automated chromatographic purification of Sr and Ca for isotopic analysis. J. Anal. At. Spectrom. 30, 1906–1912.

Ryan, B.M., Kirby, J.K., Degryse, F., Harris, H., McLaughlin, M.J., Scheiderich, K., 2013. Copper speciation and isotopic fractionation in plants: uptake and translocation mechanisms. New Phytol. 199, 367–378. https://doi.org/10.1111/nph.12276.

Ryan, B.M., Kirby, J.K., Degryse, F., Scheiderich, K., McLaughlin, M.J., 2014. Copper isotope fractionation during equilibration with natural and synthetic ligands. Environ. Sci. Technol. 48, 8620–8626. https://doi.org/10.1021/es500764x.

Sauzéat, L., Bernard, E., Perret-Liaudet, A., Quadrio, I., Vighetto, A., Krolak-Salmon, P., Broussolle, E., Leblanc, P., Balter, V., 2018. Isotopic evidence for disrupted copper metabolism in amyotrophic lateral sclerosis. iScience 6, 264–271. https://doi.org/10.1016/j.isci.2018.07.023.

Sauzéat, L., Costas-Rodríguez, M., Albalat, E., Mattielli, N., Vanhaecke, F., Balter, V., 2021. Inter-comparison of stable iron, copper and zinc isotopic compositions in six reference materials of biological origin. Talanta 221, 121576. https://doi.org/10.1016/j.talanta.2020.121576.

Savage, P.S., Moynier, F., Chen, H., Shofner, G., Siebert, J., Badro, J., Puchtel, I.S., 2015. Copper isotope evidence for large-scale sulphide fractionation during Earth's differentiation. Geochem. Perspect. Lett., 53–64 https://doi.org/10.7185/geochemlet.1506.

Schilling, K., Basu, A., Kaplan, A., Perkins, W.T., 2021. Metal distribution, bioavailability and isotope variations in polluted soils from Lower Swansea Valley, UK. Environ. Geochem. Health 43, 2899–2912. https://doi.org/10.1007/s10653-020-00794-x.

Schleicher, N.J., Dong, S., Packman, H., Little, S.H., Ochoa Gonzalez, R., Najorka, J., Sun, Y., Weiss, D.J., 2020. A global assessment of copper, zinc, and lead isotopes in mineral dust sources and aerosols. Front. Earth Sci. 8, 167. https://doi.org/10.3389/feart.2020.00167.

Schmidt, M., Leybourne, M.I., Kyser, T.K., 2017. Dendrochronology in mineral exploration: developing tools to see through anthropogenic impacts. Geochem.: Explor., Environ., Anal. 17, 357–366. https://doi.org/10.1144/geochem2017-027.

Schmitt, A.-D., Gangloff, S., Cobert, F., Lemarchand, D., Stille, P., Chabaux, F., 2009. High performance automated ion chromatography separation for Ca isotope measurements in geological and biological samples. J. Anal. At. Spectrom. 24, 1089–1097.

Seo, J.H., Lee, S.K., Lee, I., 2007. Quantum chemical calculations of equilibrium copper (I) isotope fractionations in ore-forming fluids. Chem. Geol. 243, 225–237. https://doi.org/10.1016/j.chemgeo.2007.05.025.

Shahid, M., Dumat, C., Khalid, S., Schreck, E., Xiong, T., Niazi, N.K., 2017. Foliar heavy metal uptake, toxicity and detoxification in plants: a comparison of foliar and root metal uptake. J. Hazard. Mater. 325, 36–58. https://doi.org/10.1016/j.jhazmat.2016.11.063.

Sherman, D.M., 2013. Equilibrium isotopic fractionation of copper during oxidation/reduction, aqueous complexation and ore-forming processes: predictions from hybrid density functional theory. Geochim. Cosmochim. Acta 118, 85–97. https://doi.org/10.1016/j.gca.2013.04.030.

Sherman, D.M., Little, S.H., 2020. Isotopic disequilibrium of Cu in marine ferromanganese crusts: evidence from ab initio predictions of Cu isotope fractionation on sorption to birnessite. Earth Planet. Sci. Lett. 549, 116540. https://doi.org/10.1016/j.epsl.2020.116540.

Shields, W.R., Goldich, S.S., Garner, E.L., Murphy, T.J., 1965. Natural variations in the abundance ratio and the atomic weight of copper. J. Geophys. Res. 70, 479–491.

Šillerová, H., Chrastný, V., Vítková, M., Francová, A., Jehlička, J., Gutsch, M.R., Kocourková, J., Aspholm, P.E., Nilsson, L.O., Berglen, T.F., Jensen, H.K.B., Komárek, M., 2017. Stable isotope tracing of Ni and Cu pollution in North-East Norway: potentials and drawbacks. Environ. Pollut. 228, 149–157. https://doi.org/10.1016/j.envpol.2017.05.030.

Sillitoe, R.H., 2010. Porphyry copper systems. Econ. Geol. 105, 3–41.

Souto-Oliveira, C.E., Babinski, M., Araújo, D.F., Andrade, M.F., 2018. Multi-isotopic fingerprints (Pb, Zn, Cu) applied for urban aerosol source apportionment and discrimination. Sci. Total Environ. 626, 1350–1366. https://doi.org/10.1016/j.scitotenv.2018.01.192.

Souto-Oliveira, C.E., Babinski, M., Araújo, D.F., Weiss, D.J., Ruiz, I.R., 2019. Multi-isotope approach of Pb, Cu and Zn in urban aerosols and anthropogenic sources improves tracing of the atmospheric pollutant sources in megacities. Atmos. Environ. 198, 427–437. https://doi.org/10.1016/j.atmosenv.2018.11.007.

Stengle, J.M., Schade, A.L., 1957. Diurnal-nocturnal variations of certain blood constituents in normal human subjects: plasma iron, siderophilin, bilirubin, copper, total serum protein and albumin, haemoglobin and haematocrit. Br. J. Haematol. 3, 117–124. https://doi.org/10.1111/j.1365-2141.1957.tb05778.x.

Su, J., Mathur, R., Brumm, G., D'Amico, P., Godfrey, L., Ruiz, J., Song, S., 2018. Tracing copper migration in the Tongling area through copper isotope values in soils and waters. Int. J. Environ. Res. Public Health 15, 2661. https://doi.org/10.3390/ijerph15122661.

Sullivan, K., Layton-Matthews, D., Leybourne, M., Kidder, J., Mester, Z., Yang, L., 2020a. Copper isotopic analysis in geological and biological reference materials by MC-ICP-MS. Geostand. Geoanal. Res. 44, 349–362. https://doi.org/10.1111/ggr.12315.

Sullivan, K., Moore, R.E.T., Rehkämper, M., Layton-Matthews, D., Leybourne, M.I., Puxty, J., Kyser, T.K., 2020b. Postprandial zinc stable isotope response in human blood serum. Metallomics 9, 1380–1388. https://doi.org/10.1039/D0MT00122H.

Takano, S., Tanimizu, M., Hirata, T., Sohrin, Y., 2013. Determination of isotopic composition of dissolved copper in seawater by multi-collector inductively coupled plasma mass spectrometry after pre-concentration using an ethylenediaminetriacetic acid chelating resin. Anal. Chim. Acta 784, 33–41. https://doi.org/10.1016/j.aca.2013.04.032.

Takano, S., Tanimizu, M., Hirata, T., Sohrin, Y., 2014. Isotopic constraints on biogeochemical cycling of copper in the ocean. Nat. Commun. 5, 5663. https://doi.org/10.1038/ncomms6663.

Takano, S., Tanimizu, M., Hirata, T., Shin, K.-C., Fukami, Y., Suzuki, K., Sohrin, Y., 2017. A simple and rapid method for isotopic analysis of nickel, copper, and zinc in seawater using chelating extraction and anion exchange. Anal. Chim. Acta 967, 1–11. https://doi.org/10.1016/j.aca.2017.03.010.

Takano, S., Liao, W.-H., Tian, H.-A., Huang, K.-F., Ho, T.-Y., Sohrin, Y., 2020. Sources of particulate ni and cu in the water column of the northern South China Sea: evidence from elemental and isotope ratios in aerosols and sinking particles. Mar. Chem. 219, 103751. https://doi.org/10.1016/j.marchem.2020.103751.

Takano, S., Tsuchiya, M., Imai, S., Yamamoto, Y., Fukami, Y., Suzuki, K., Sohrin, Y., 2021. Isotopic analysis of nickel, copper, and zinc in various freshwater samples for source identification. Geochem. J. 55, 171–183.

Tanzi, R.E., Petrukhin, K., Chernov, I., Pellequer, J.L., Wasco, W., Ross, B., Romano, D.M., Parano, E., Pavone, L., Brzustowicz, L.M., 1993. The Wilson disease gene is a copper transporting ATPase with homology to the menkes disease gene. Nat. Genet. 5, 344.

Télouk, P., Puisieux, A., Fujii, T., Balter, V., Bondanese, V.P., Morel, A.-P., Clapisson, G., Lamboux, A., Albarede, F., 2015. Copper isotope effect in serum of cancer patients.A pilot study. Metallomics 7, 299–308. https://doi.org/10.1039/C4MT00269E.

Télouk, P., Plissonnier, M.-L., Merle, P., Zoulim, F., Fares, N., Guilloreau, P., Parent, R., Bacchetta, J., Danan, M., Carandina, S., 2022. Copper isotope evidence of oxidative stress-induced hepatic breakdown and the transition to hepatocellular carcinoma. Gastro Hep Adv. 1, 480–486.

Tennant, A., Rauk, A., Wieser, M.E., 2017. Computational modelling of the redistribution of copper isotopes by proteins in the liver. Metallomics 9, 1809–1819. https://doi.org/10.1039/C7MT00248C.

Thapalia, A., Borrok, D.M., Van Metre, P.C., Musgrove, M., Landa, E.R., 2010. Zn and Cu isotopes as tracers of anthropogenic contamination in a sediment core from an urban lake. Environ. Sci. Technol. 44, 1544–1550. https://doi.org/10.1021/es902933y.

Toubhans, B., Gourlan, A.T., Telouk, P., Lutchman-Singh, K., Francis, L.W., Conlan, R.S., Margarit, L., Gonzalez, D., Charlet, L., 2020. Cu isotope ratios are meaningful in ovarian cancer diagnosis. J. Trace Elem. Med. Biol. 62, 126611. https://doi.org/10.1016/j.jtemb.2020.126611.

Turnlund, J.R., Scott, K.C., Peiffer, G.L., Jang, A.M., Keyes, W.R., Keen, C.L., Sakanashi, T.M., 1997. Copper status of young men consuming a low-copper diet. Am. J. Clin. Nutr. 65, 72–78. https://doi.org/10.1093/ajcn/65.1.72.

Uauy, R., Olivares, M., Gonzalez, M., 1998. Essentiality of copper in humans. Am. J. Clin. Nutr. 67, 952S–959S.

Van Heghe, L., Engström, E., Rodushkin, I., Cloquet, C., Vanhaecke, F., 2012. Isotopic analysis of the metabolically relevant transition metals Cu, Fe and Zn in human blood from vegetarians and omnivores using multi-collector ICP-mass spectrometry. J. Anal. At. Spectrom. 27, 1327–1334. https://doi.org/10.1039/c2ja30070b.

Van Heghe, L., Deltombe, O., Delanghe, J., Depypere, H., Vanhaecke, F., 2014. The influence of menstrual blood loss and age on the isotopic composition of Cu, Fe and Zn in human whole blood. J. Anal. At. Spectrom. 29, 478–482.

Vance, D., Archer, C., Bermin, J., Perkins, J., Statham, P.J., Lohan, M.C., Ellwood, M.J., Mills, R.A., 2008. The copper isotope geochemistry of rivers and the oceans. Earth Planet. Sci. Lett. 274, 204–213. https://doi.org/10.1016/j.epsl.2008.07.026.

Vance, D., Matthews, A., Keech, A., Archer, C., Hudson, G., Pett-Ridge, J., Chadwick, O.A., 2016. The behaviour of Cu and Zn isotopes during soil development: controls on the dissolved load of rivers. Chem. Geol. 445, 36–53. https://doi.org/10.1016/j.chemgeo.2016.06.002.

Vanhaecke, F., Costas-Rodríguez, M., 2021. High-precision isotopic analysis of essential mineral elements: capabilities as a diagnostic/prognostic tool. View 2, 20200094. https://doi.org/10.1002/VIW.20200094.

Viers, J., Grande, J.A., Zouiten, C., Freydier, R., Masbou, J., Valente, T., de la Torre, M.-L., Destrigneville, C., Pokrovsky, O.S., 2018. Are Cu isotopes a useful tool to trace metal sources and processes in acid mine drainage (AMD) context? Chemosphere 193, 1071–1079. https://doi.org/10.1016/j.chemosphere.2017.11.133.

Walker, E.C., Cuttitta, F., Senftle, F.E., 1958. Some natural variations in the relative abundance of copper isotopes. Geochim. Cosmochim. Acta 15, 183–194.

Wang, Z., Chen, J., Zhang, T., 2017. Cu isotopic composition in surface environments and in biological systems: a critical review. Int. J. Environ. Res. Public Health 14. https://doi.org/10.3390/ijerph14050538.

Wang, Q., Zhou, L., Feng, L., Liu, Jincun, Liu, Jinhua, J. Algeo, T., Yang, L., 2020. Use of a Cu-selective resin for Cu preconcentration from seawater prior to its isotopic analysis by MC-ICP-MS. J. Anal. At. Spectrom. 35, 2732–2739. https://doi.org/10.1039/D0JA00096E.

Wang, Q., Zhou, L., Little, S.H., Liu, J., Feng, L., Tong, S., 2020b. The geochemical behavior of Cu and its isotopes in the Yangtze River. Sci. Total Environ. 728, 138428. https://doi.org/10.1016/j.scitotenv.2020.138428.

Wang, L., Jin, Y., Weiss, D.J., Schleicher, N.J., Wilcke, W., Wu, L., Guo, Q., Chen, J., O'Connor, D., Hou, D., 2021. Possible application of stable isotope compositions for the identification of metal sources in soil. J. Hazard. Mater. 407, 124812. https://doi.org/10.1016/j.jhazmat.2020.124812.

Wang, R.-R., Yu, H.-M., Cheng, W.-H., Liu, Y.-C., Zhang, G.-L., Li, D.-C., Huang, F., 2022. Copper migration and isotope fractionation in a typical paddy soil profile of the Yangtze Delta. Sci. Total Environ. 821, 153201. https://doi.org/10.1016/j.scitotenv.2022.153201.

Wang, W., Liu, X., Zhang, C., Sheng, F., Song, S., Li, P., Dai, S., Wang, B., Lu, D., Zhang, L., Yang, X., Zhang, Z., Liu, S., Zhang, A., Liu, Q., Jiang, G., 2022. Identification of two-dimensional copper signatures in human blood for bladder cancer with machine learning. Chem. Sci. https://doi.org/10.1039/D1SC06156A 10.1039.D1SC06156A.

Warburg, O., 1956. On the origin of cancer cells. Science 123, 309–314. https://doi.org/10.1126/science.123.3191.309.

Weinstein, C., Moynier, F., Wang, K., Paniello, R., Foriel, J., Catalano, J., Pichat, S., 2011. Isotopic fractionation of Cu in plants. Chem. Geol. 286, 266–271. https://doi.org/10.1016/j.chemgeo.2011.05.010.

Wiederhold, J.G., 2015. Metal stable isotope signatures as tracers in environmental geochemistry. Environ. Sci. Technol. 49, 2606–2624. https://doi.org/10.1021/es504683e.

Wiggenhauser, M., Moore, R.E.T., Wang, P., Bienert, G.P., Laursen, K.H., Blotevogel, S., 2022. Stable isotope fractionation of metals and metalloids in plants: a review. Front. Plant Sci. 13.

Wu, S., Zheng, Y., Wang, D., Chang, H., Tan, M., 2017. Variation of copper isotopes in chalcopyrite from Dabu porphyry Cu-Mo deposit in Tibet and implications for mineral exploration. Ore Geol. Rev. 90, 14–24. https://doi.org/10.1016/j.oregeorev.2017.10.001.

Yang, L., Tong, S., Zhou, L., Hu, Z., Mester, Z., Meija, J., 2018. A critical review on isotopic fractionation correction methods for accurate isotope amount ratio measurements by MC-ICP-MS. J. Anal. At. Spectrom. https://doi.org/10.1039/C8JA00210J.

Yang, S.-C., Hawco, N.J., Pinedo-González, P., Bian, X., Huang, K.-F., Zhang, R., John, S.G., 2020. A new purification method for Ni and Cu stable isotopes in seawater provides evidence for widespread Ni isotope fractionation by phytoplankton in the North Pacific. Chem. Geol. 547, 119662. https://doi.org/10.1016/j.chemgeo.2020.119662.

Yang, Z., Jackson, S.E., Skulski, T., 2021. Characterization of four copper materials for application as reference materials for high precision copper isotope analysis by laser ablation inductively coupled plasma multi-collector mass spectrometry. Front. Chem. https://doi.org/10.3389/fchem.2021.617205.

Yruela, I., 2005. Copper in plants. Braz. J. Plant Physiol. 17, 145–156. https://doi.org/10.1590/S1677-04202005000100012.

Zeng, J., Han, G., 2020. Preliminary copper isotope study on particulate matter in Zhujiang River, southwest China: application for source identification. Ecotoxicol. Environ. Saf. 198, 110663. https://doi.org/10.1016/j.ecoenv.2020.110663.

Zhang, Y., Bao, Z., Lv, N., Chen, K., Zong, C., Yuan, H., 2020. Copper isotope ratio measurements of Cu-dominated minerals without column chromatography using MC-ICP-MS. Front. Chem. 8. https://doi.org/10.3389/fchem.2020.00609.

Zhao, Y., Xue, C., Liu, S.-A., Symons, D.T.A., Zhao, X., Yang, Y., Ke, J., 2017. Copper isotope fractionation during sulfide-magma differentiation in the Tulaergen magmatic Ni–Cu deposit, NW China. Lithos 286–287, 206–215. https://doi.org/10.1016/j.lithos.2017.06.007.

Zheng, S.J., He, Y.F., Arakawa, Y., Masaoka, Y., Tang, C., 2005. A copper-deficiency-induced root reductase is different from the iron-deficiency-induced one in red clover (Trifolium pratense L.). Plant Soil 273, 69–76. https://doi.org/10.1007/s11104-004-6825-1.

Zhu, X.K., O'Nions, R.K., Guo, Y., Belshaw, N.S., Rickard, D., 2000. Determination of natural Cu-isotope variation by plasma-source mass spectrometry: implications for use as geochemical tracers. Chem. Geol. 163, 139–149. https://doi.org/10.1016/S0009-2541(99)00076-5.

Zhu, X.K., Guo, Y., Williams, R.J.P., O'Nions, R.K., Matthews, A., Belshaw, N.S., Canters, G.W., de Waal, E.C., Weser, U., Burgess, B.K., Salvato, B., 2002. Mass fractionation processes of transition metal isotopes. Earth Planet. Sci. Lett. 200, 47–62. https://doi.org/10.1016/S0012-821X(02)00615-5.

Zhu, X.K., Li, S.Z., Luo, Y.M., Wu, L.H., 2010. Copper isotope fractionation by higher plants. Geochimica et Cosmochimica Acta. Ergamon-Elsevier Science Ltd., p. A1234.